AD NUMBER: AD0829842
LIMITATION CHANGES
TO: Approved for public release; distribution is unlimited.
FROM: Distribution authorized to U.S. Government agencies and their contractors only; Export Control; 30 Mar 1968. Other requests shall be referred to Commanding Officer, Naval Weapons Center Corona Laboratories (Code 2035), Corona, CA 91720.
AUTHORITY
USNWC ltr 24 Mar 1972

NWCCL TP 759

AN EVALUATION OF VLF DAYTIME PROPAGATION PARAMETERS USING A MULTI-FREQUENCY SOUNDER

by

V. E. Hildebrand
D. G. Morfitt

Research Department

ABSTRACT. An oblique incidence VLF ionospheric sounder system developed at the Naval Weapons Center Corona Laboratories gives a means of obtaining multi-frequency amplitude and phase measurements in the VLF band simultaneously at up to 10 frequencies over a single propagation path. The analysis presented in this report is an attempt (1) to determine the degree of correlation obtainable between experimental sounder data and predicted results from existing theoretical models for VLF propagation, (2) to determine the variability of propagation parameters derived from the experimental data, and (3) to compare theoretical model parameters which best describe experimental results with previously published findings.

The propagation path chosen was from Hilo, Hawaii to Lucerne Valley, Southern California (4,166 km). The experimental data was obtained during March 1967.

NAVAL WEAPONS CENTER
CORONA LABORATORIES, CORONA, CALIFORNIA • MARCH 1968

DISTRIBUTION STATEMENT

THIS DOCUMENT IS SUBJECT TO SPECIAL EXPORT CONTROLS AND EACH TRANSMITTAL TO FOREIGN GOVERNMENTS OR FOREIGN NATIONALS MAY BE MADE ONLY WITH PRIOR APPROVAL OF THE COMMANDING OFFICER OF THE NAVAL WEAPONS CENTER CORONA LABORATORIES (CODE 2035), CORONA, CALIFORNIA 91720.

71

CONTENTS

Introduction 1
Background 2
General Features of the Data 5
Theoretical Propagation Models 14
Experimental and Analytical Procedures 28
Evaluation Results 37
Discussion 52
Conclusions 62
References 64

ACKNOWLEDGMENTS

The authors wish to acknowledge the efforts of Mr. Fred Bickford of the Electronics Division, who was in charge of field test measurements, and to personnel of the Astrophysics Research Corporation, who participated in the field tests.

BLANK PAGE

INTRODUCTION

A special purpose very low frequency (VLF) oblique sounder system has been developed at the Naval Weapons Center (NWC) Corona Laboratories which, in conjunction with highly refined analytical techniques, provides a major advance in the capability for determining those parameters pertinent to VLF propagation. This sounder system was developed under the sponsorship of the Defense Communications Agency (DCA) and has been primarily utilized to obtain propagation data over a path from Hawaii to Southern California. Most of the data evaluation has been undertaken as part of a project sponsored by the Defense Atomic Support Agency (DASA). The experience gained to date has demonstrated that a wealth of information detail previously not obtainable can be readily acquired by this means, thus permitting a much more definitive determination of signal propagation parameters.

The detailed information that is derivable from the data obtained with this system is so extensive that one is forced to work with selected parts of it. Consequently, as an initial effort an attempt has been made to evaluate the daytime propagation parameters of a low-altitude overwater generally eastward propagation path. The path was chosen partly for convenience and partly because much data is available for comparison from previous measurements on very similar paths. The daytime period was chosen because of its relatively high stability and repeatability of propagation conditions and because previous investigators in general have obtained the best correlation between propagation models and experimental findings during daytime. The March 1967 test series provided the first opportunity to obtain enough data to make a comparative evaluation of the type undertaken in this report. Even then, since it was decided to investigate a few specific transmission periods in rather great detail, the amount of propagation data considered was limited with respect to time. Because of this it cannot be stated with any definiteness that the derived propagation parameters are truly representative of the equinox period.

The established objectives in evaluating this daytime propagation data were (1) to determine the degree of correlation obtainable between experimental data and model prediction, (2) to determine the variability of propagation parameters derived from the experimental data, and (3) to compare with previously published findings the theoretical model parameters which best describe experimental results.

Since this is the first report covering the evaluation of VLF propagation parameters using a multi-frequency sounder, a general discussion of the sounder features and the data evaluation techniques will be presented before examining the details of the daytime propagation data.

BACKGROUND

A detailed description of the multi-frequency VLF ionospheric sounder system has been presented in a previous report (Ref. 1). Briefly, the system consists of 10-frequency, time-shared transmitter and receiver as shown in Fig. 1. The oblique sounder system is portable in the sense that the equipment can be set up to collect data over any path where sufficient space is available at the terminators to construct the transmitting and receiving antenna and where the terrain conductivity at the transmitter terminal is sufficiently low to obtain adequate antenna efficiency. The transmitting antenna consists of parallel multiple conductors laid on the surface much as one would lay a field telephone line. The antenna design (Ref. 2 and 3) is especially configured for the requirements of the measurements and the characteristics of the construction site. The sounder system has been used to collect propagation data over a path from Hawaii to Southern California and from Southern Brazil to Central Bolivia. The transmitter site in Hawaii is located approximately 42 km west of Hilo, Hawaii. The receiver can be set up at any convenient location which provides sufficient room for the superdirective receiving antenna array (Ref. 4). Normally, about one mile separation is used for a two-loop array. The receiving site utilized in the propagation tests to be described in this report was located at the Corona Laboratories field site near Lucerne Valley, California. The propagation path from Hawaii to this field site is shown in Fig. 2. The cross located in the lower central part of this figure is the position of the subsolar point at midpath noon for the equinox period.

The transmitter transmits short segments of each of 10 frequencies in sequence; the length of each frequency segment can be as short as 320 μsec, which is only 3 cycles of the lowest frequency. In normal operation these groups of 10 frequencies are repeated continuously, giving a 10-percent duty cycle for each frequency. The correlation receivers at the receiver site are gated on in the same sequence as

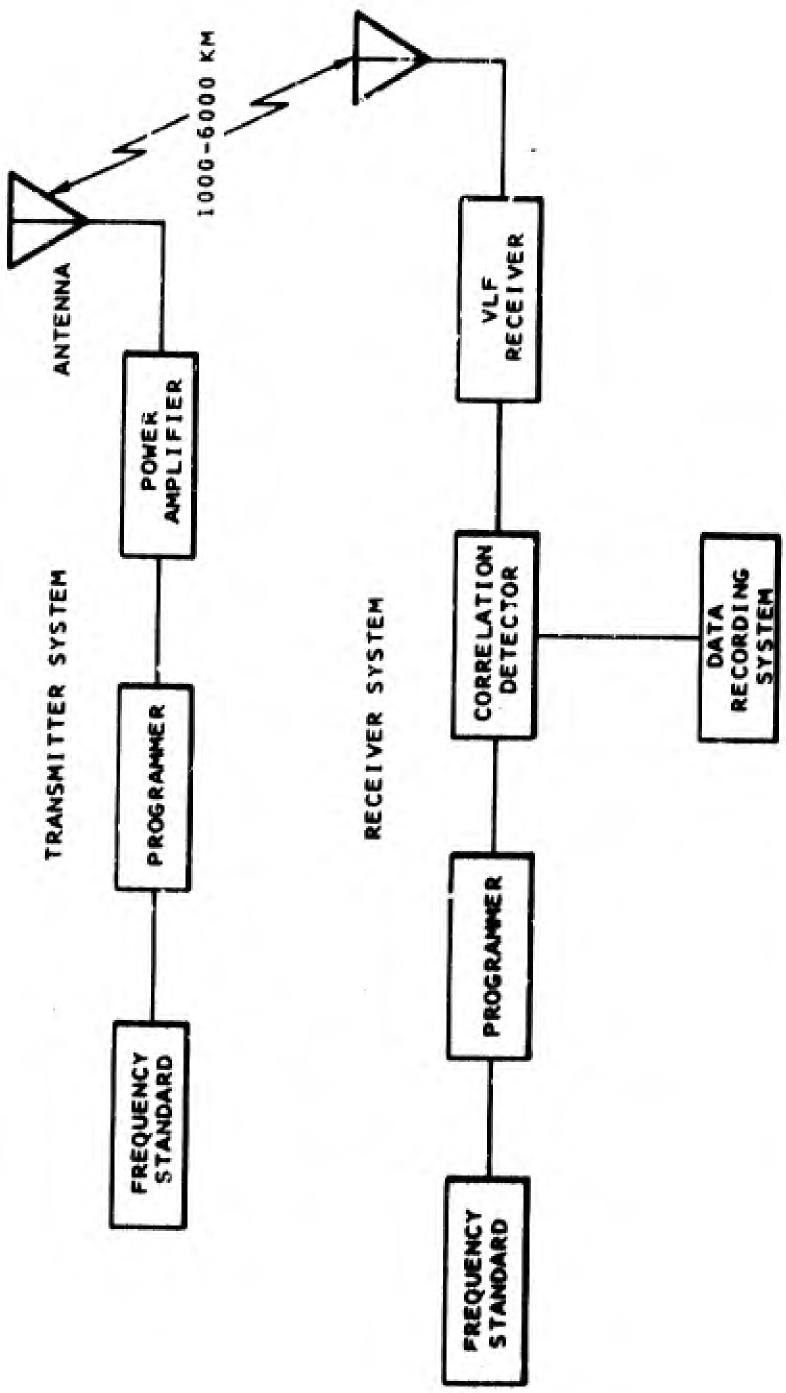

FIG. 1. Block Diagram of Transmit/Receive Systems.

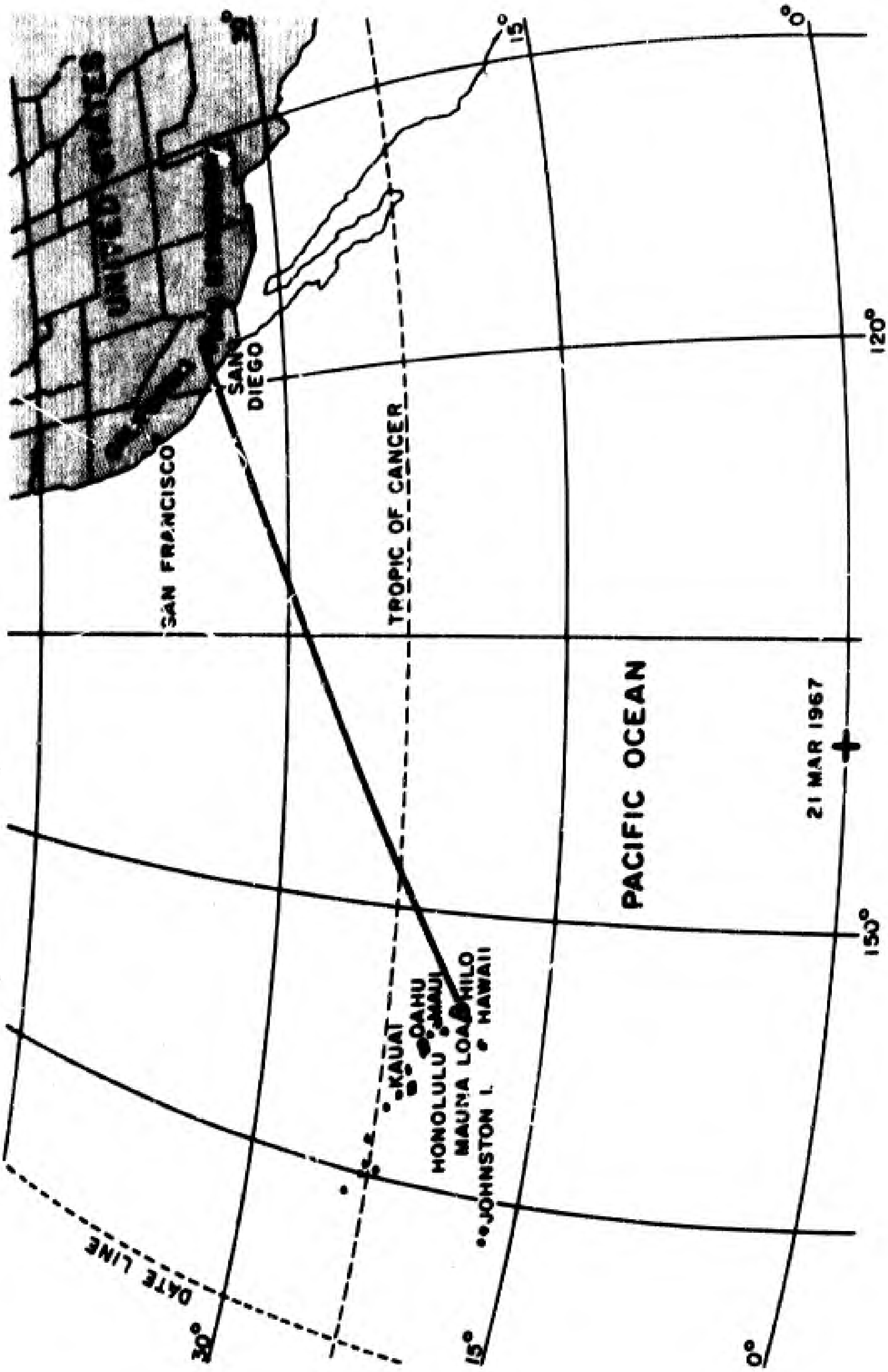

FIG. 2. VLF Propagation Path Between Hawaii and California.

the transmitter pulses, and a variable delay is available for the local receiver reference signals so that synchronization of the transmitter and receiving system can be achieved. Both transmitter and receiver are controlled by rubidium frequency standards so that synchronization can be maintained over long periods of time. Transmitted frequencies are normally in the range from 9.375 kHz to 31.25 kHz. The Corona Laboratories are presently tasked by DCA to extend the oblique sounder capability to 60 kHz. The correlation detection technique utilized in the receiver system, along with the noise discrimination features of the superdirective receiving antenna makes it possible to detect very low level signals and still maintain high measurement accuracy. Both the field strength and received phase are measured.

The propagation data to be discussed in this report was acquired during a test series conducted in March 1967. The propagation path from the transmitter on the island of Hawaii (155.60°W, 19.642°N) to the receiver in Southern California (116.625°W, 34.533°N) was 4.166 megameters in length; its midpath point (137.47°W, 28.48°N) has a magnetic field strength of 0.425 gauss and a magnetic dip angle of 50°. The midpath magnetic field angle with respect to the path of propagation (magnetic azimuth) is 50.6°.

All data is recorded on digital magnetic tape so that with computer processing all or any portion of the data can be plotted to any desired scale in any format. In addition, the digital data can be further filtered, if necessary, to improve signal to noise ratios.

GENERAL FEATURES OF THE DATA

Transmissions typically ran for a 30-hr period so that the data exists in 30-hr segments of continuous information. The tests were started prior to midpath noon and ended shortly after midpath noon. These start and stop times were selected to take advantage of the more stable periods of signal propagation in order to achieve the greatest accuracy in equipment calibration.

Samples of the received signal amplitude at each of the 10 frequencies covering the 30-hr period are shown in Fig. 3(a), (b), and (c). Data for two test periods covering the 7th and 14th of March are shown to provide a comparison. The data has been normalized for an equivalent radiated power of 1 kW. A vertical bar in the upper right hand

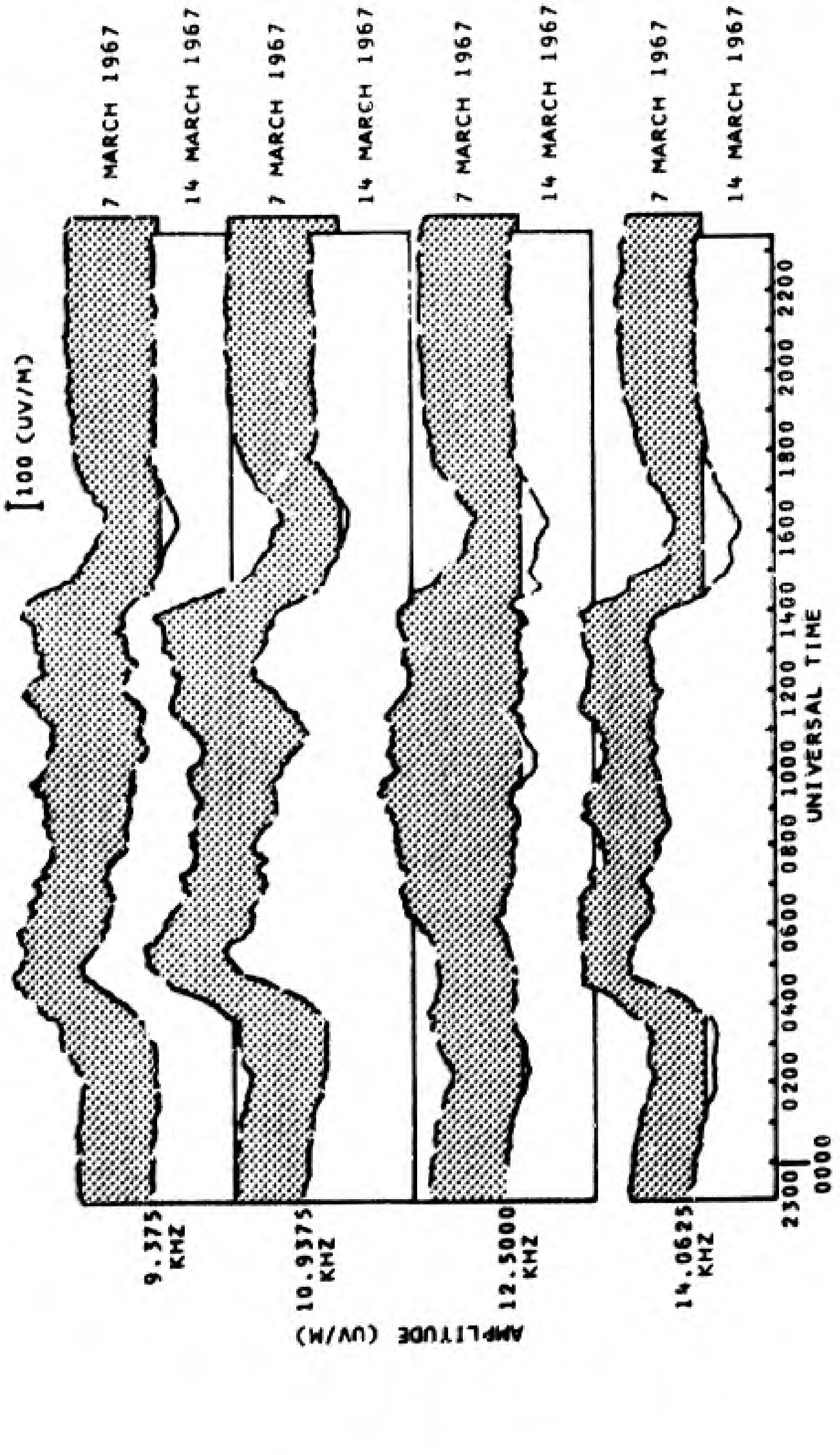

FIG. 3(a). Amplitude of Received Signals (9.3 to 14.06 kHz).

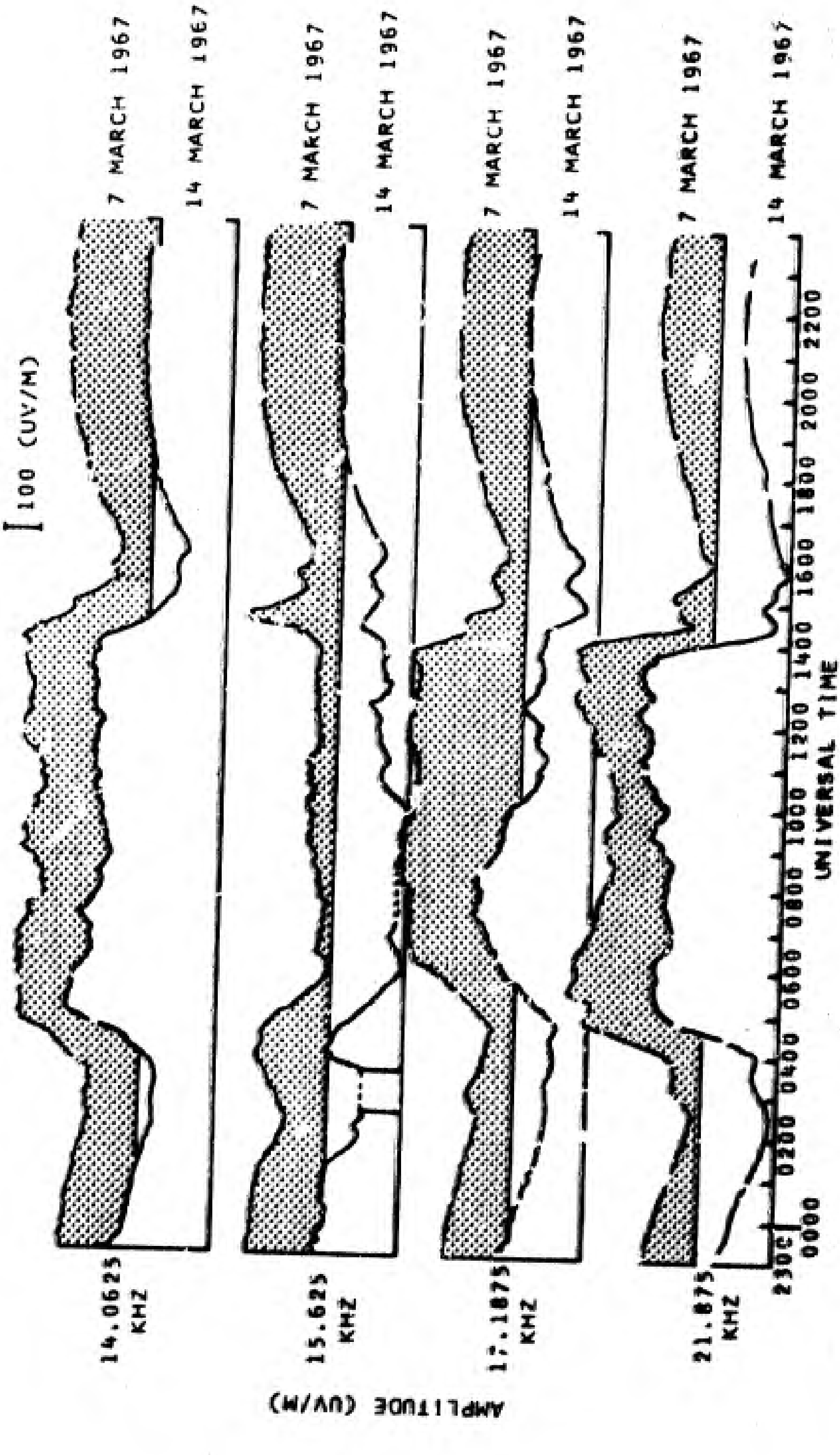

FIG. 3(b). Amplitude of Received Signals (14.6 to 21.8 kHz).

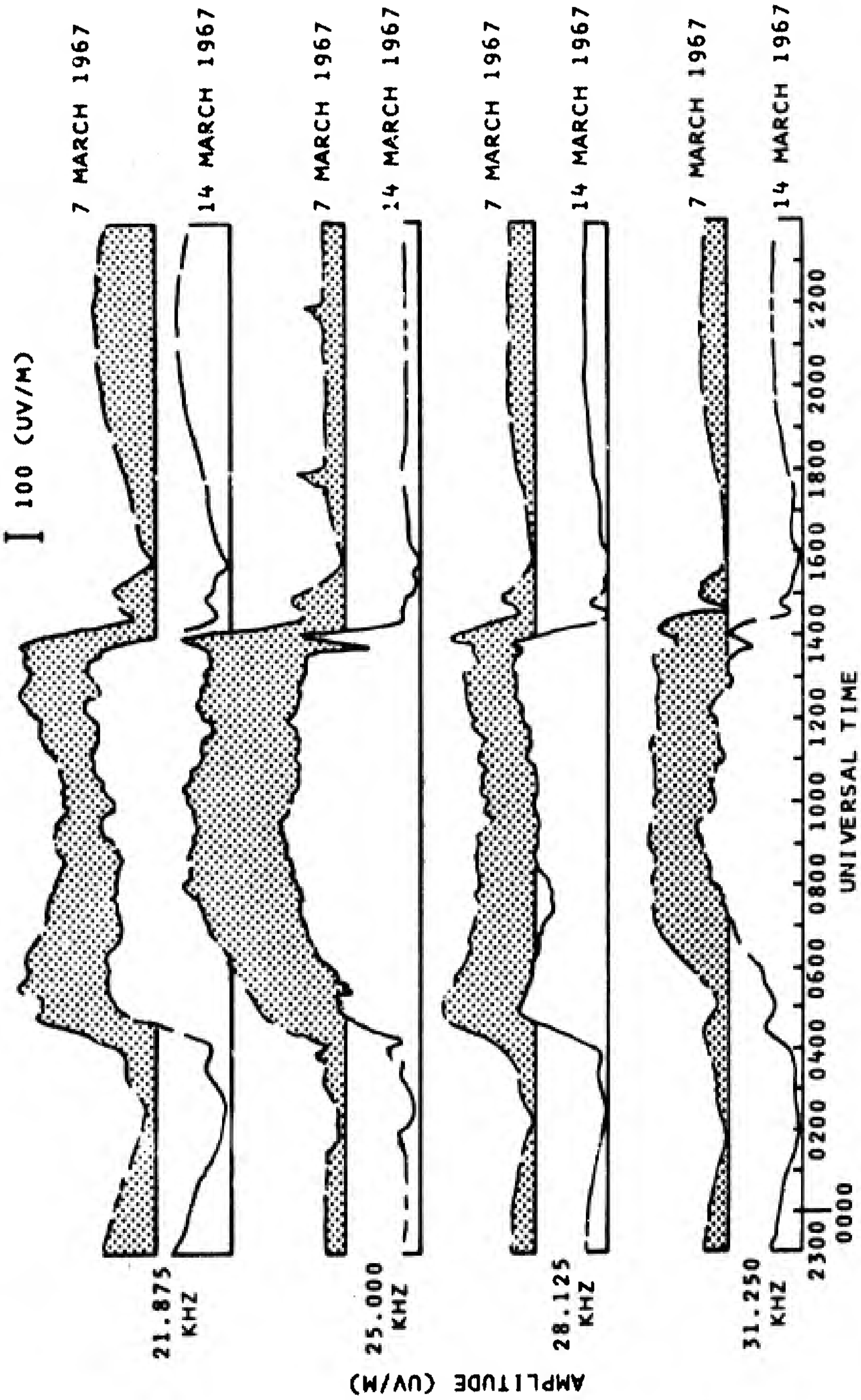

FIG. 3(c). Amplitude of Received Signals (21.8 to 31.2 kHz).

corner of each figure indicates the amplitude scale. The sunset transition occurs in the interval around 0320 universal time; the sunrise transition occurs in the interval around 1515. The path is thus totally in daylight from 1630 to the following day at about 0200. Likewise, the path is in total darkness from 0440 to 1345. Both the day and nighttime signal levels are generally high at the lower VLF frequencies, the variability between day and night increasing with frequency. The signal levels during daytime are characterized at the lowest VLF frequencies by a constant signal level in contrast to a continuously varying signal at a higher frequency. This signal variability throughout the day increases with increased frequency to 21.875 kHz. The signal level at 25 kHz is very low during the entire day due to severe modal interference occurring at the 4.166 megameter distance. The signal levels at 21.125 and 31.250 kHz are also relatively weak because of modal interference, although it is not as severe as at the 25 kHz frequency. Some interference is encountered in the reception of the 25 kHz signal; this interference is evidenced by the marked signal increases centered around 1800 and just prior to 2200.

Nighttime propagation at all frequencies is significantly more variable than daytime propagation. It is noted in the 7 March nighttime data that there is a characteristic progression with frequency from the saucer-shaped curve with maximum depression near 0900 to an arch-shaped curve having a related maximum at 0900. This characteristic feature is interrupted by a very weak signal level existing at 15.625 kHz caused by pronounced modal destructive interference. The modal destructive interference at 15.625 kHz was most severe around 0600, becoming somewhat less severe for the rest of the nighttime period on 7 March. The frequency of maximum constructive modal interference occurs near 25 kHz for the nighttime propagation parameters. An easily recognized feature of the nighttime propagation data is the differences in the time behavior of the received signals for the two dates. The symmetry of the data for the 7 March period is not repeated in the 14 March data; rather, what appears to be an abrupt change in propagation parameters starts at 0800, the change being continuous through the sunrise transition. This effect is most evident at the 15.6 and 17.18 kHz frequencies; the 15.6 kHz signal appears to drift out of the severe modal interference condition, whereas the 17.18 kHz signal begins a gradual but marked signal decrease, probably evidence of increasing modal interference. The resulting differences in propagation characteristics are also quite evident at the other frequencies.

The sunset and sunrise transition times have very interesting features which vary with frequency, being generally much more pronounced at the higher frequencies. It is particularly interesting to note the time variability of the nighttime signal buildup at the higher frequencies. The sunrise-associated signal fades are quite marked at the higher frequencies, and occur at progressively later times with decreasing frequency.

The received phase for these same transmissions shown in Fig. 4(a), (b), and (c) also has a number of characteristic features. For example, at the lowest frequencies during the daytime the phase is continuously varying with time, whereas at the higher frequencies the phase is relatively constant with time. The characteristics for the received phase for nighttime propagation conditions are also more variable than for the daytime as evidenced by the data on the two different days. The nighttime variability of the 15.6 kHz signal is partially due to the low signal to noise ratio existing at that time. The variability in propagation conditions evidenced in the signal amplitude data can also be observed in the phase data. Likewise, the features of the received phase during the sunrise and sunset transition periods become progressively more complex as frequency increases. The points of inflection in the phase records correspond in time with the occurrence of signal amplitude relative minima during both the sunset and sunrise transition periods. The phase reversal during the sunrise transition previously reported by a number of investigators is very evident at several of the higher VLF frequencies. It is interesting to note that once phase reversal takes place as frequency increases, this condition is not necessarily maintained. Another interesting feature of the phase data is the magnitude of the diurnal phase change with frequency, this having a relative minimum near 17 kHz. This observation is in qualitative agreement with modal theory (Ref. 5) and observation as reported by Blackband (Ref. 6).

Many of the general features presented here in a qualitative manner are presently being evaluated for a quantitative assessment of various theoretical models that have been described in the literature. One aspect of this evaluation, that of determining the VLF daytime propagation parameters, will be presented in a later section of this report.

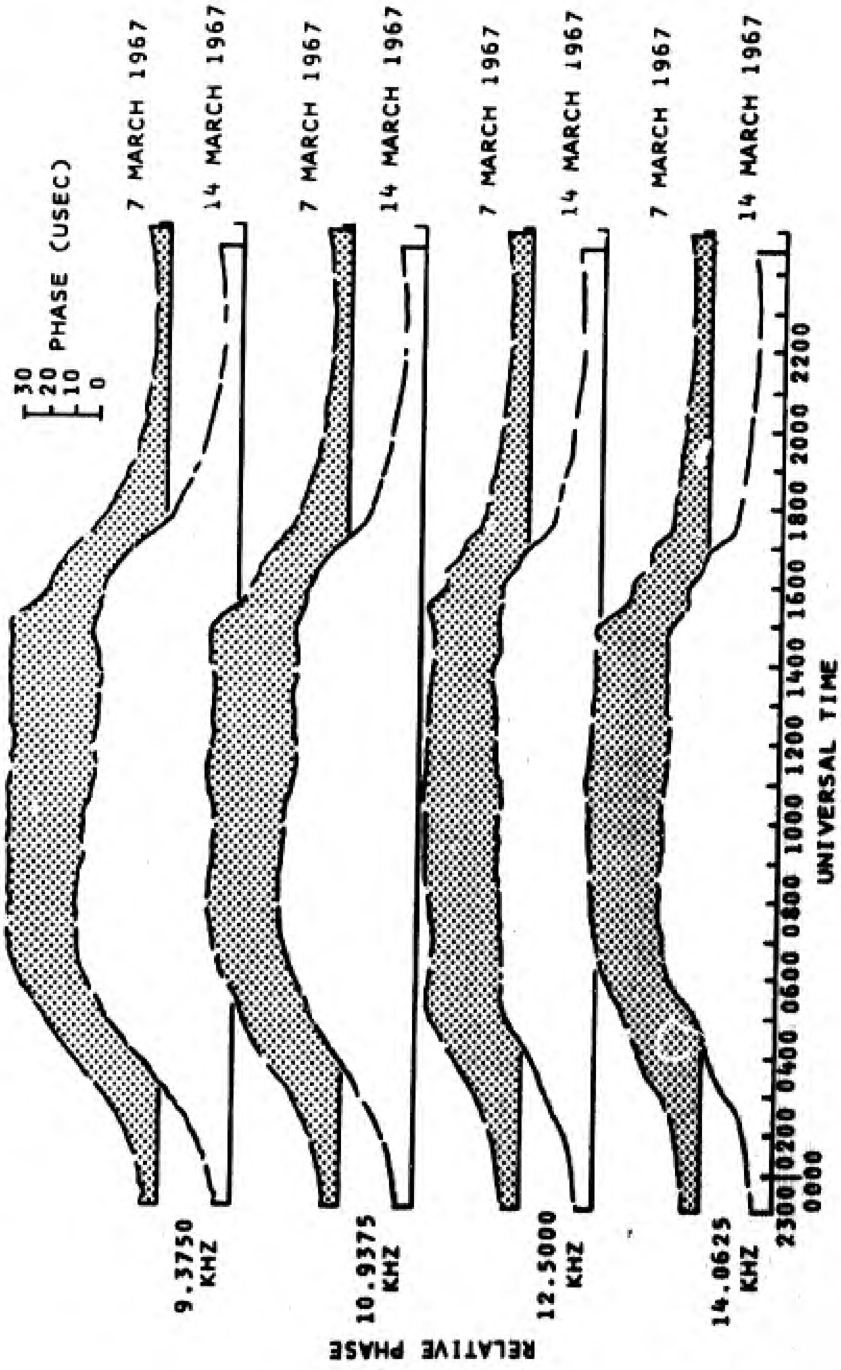

FIG. 4(a). Phase of Received Signals (9.3 to 14.06 kHz).

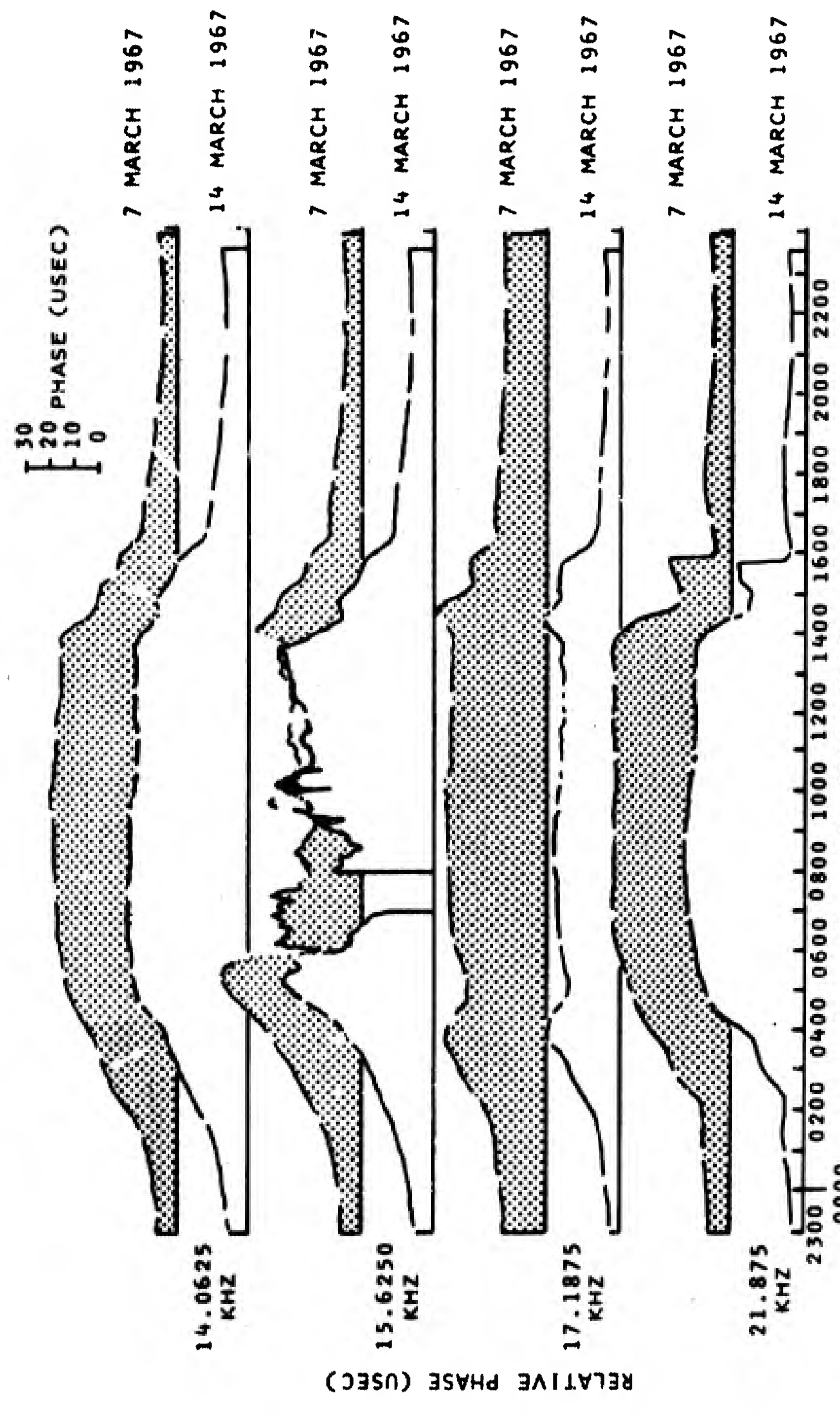

FIG. 4(b). Phase of Received Signals (14.06 to 21.8 kHz).

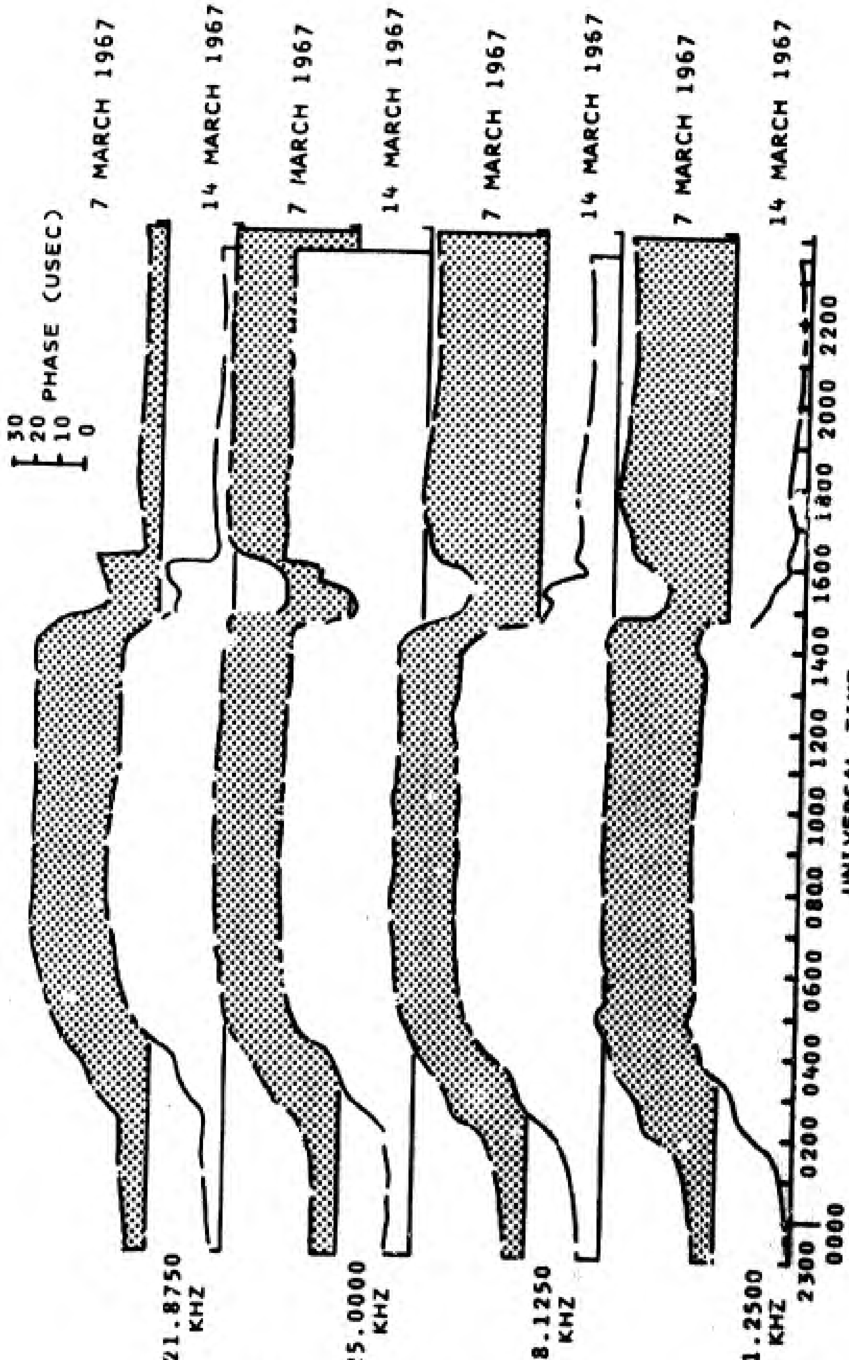

FIG. 4(c). Phase of Received Signals (21.8 to 31.25 kHz).

THEORETICAL PROPAGATION MODELS

The present state of the art of VLF propagation theory does not allow one to derive propagation parameters directly from VLF propagation data. Rather, one must assume a VLF propagation model which includes a choice of an electron density profile (electron density vs. height) and then compute the received fields for the propagation path. Several theoretical models have been developed for this purpose, most of which involve major simplifications concerning the properties of the propagation media and/or mathematical approximations which significantly limit the geophysical conditions for which such models are valid. Even the most detailed models, all of which require machine calculation, have significant limitations in the degree of complexity of the propagation environment which can be handled. Part of the long-range objective in this VLF propagation evaluation project is to determine the degree of complexity required in a VLF propagation model to adequately describe propagation conditions in different types of environments. Two computer programs have been adapted at the NWC Corona Laboratories for making theoretical calculations of VLF incident fields. Both of these programs have been generously provided to the Corona Laboratories together with assistance in adapting these programs to the Corona Laboratories computer—assistance which has been very much appreciated. One of these programs, WAVEHOP, which was developed by Berry and Chrisman (Ref. 7), calculates the electric fields at any distance from a transmitter as a series of wavehops. Inputs to the program are electron density vs. height, magnitude and dip of the magnetic field, magnetic direction of propagation, frequency, ground conductivity, ground dielectric constant, and distance. An assumed collision frequency profile is contained in the program. The output is the amplitude and phase of a ground wave and up to five wavehops along with their vector sum (the total field). Also available as output are reflection and transmission coefficients of the ionosphere for any angle of incidence.

The second program, FULLWAVE, was developed by Inoue and Horowitz (Ref. 8) and is used primarily for calculation at vertical or near vertical incidence. Inputs to this program are electron density, collision frequency, and magnetic field vs. height, the incident field from below the ionosphere, and the step size for integration. Four independent solutions to the wave equations are obtained at all heights and then combined at the boundary to match the incident conditions. Outputs from the program are phase and amplitudes of four characteristic waves, the upgoing and downgoing components of the field, the peak and average values of the total fields, and coupling coefficients between the characteristic waves. Also available are the Appleton-Hartree parameters X, Y, Z, and the index of refraction for each characteristic wave. Reflection coefficients can be obtained from ratios between various components of the downgoing and upgoing fields. All these quantities are calculated as functions of height so that the program has a "wave tracing" capability. This feature is valuable in that it allows a study of the behavior of the waves within the ionosphere so that critical heights and reception regions can be discovered and the effects of changing ionosphere profiles can be studied in detail.

Various ionospheric profiles of electron density vs. height have been suggested in the literature. Among them are the daytime exponential ionospheres described by Wait (Ref. 9) and a series of complex profiles published by Deeks (Ref. 10). The most commonly referenced of the exponential ionospheres are known as $\beta = 0.5$ and $\beta = 0.3$. Variations of the exponential profile have been used in this evaluation which may be related to Wait's notation as follows: if a profile is labeled as $\beta = 0.5$ (-3 km), the meaning is that the values of the electron density for a series of heights described by the profile $\beta = 0.5$ were given respectively to a series of heights 3 km lower.

These programs, WAVEHOP and FULLWAVE, can be used in conjunction with the experimental sounder data to deduce ionospheric profiles in the following manner. An initial estimate is made for the input profiles and the fields are calculated; these calculated fields are compared with the experimentally measured fields and differences noted. If the differences are significant, the theoretical fields are recalculated with different profiles. This trial and error pro[illegible]on-tinues until good agreement is obtained between calcu[illegible]sured fields. Past experience seems to be the best guide for [illegible]nges in the profiles to try to resolve differences at any sta[illegible] cess. Generally, it has been found expedient to assu[illegible]ially increasing electron gradient for the first attempt to m[illegible]phere profile. Once the best height for a profile is obtained, the [illegible]ep is to modify the profile from the exponential form to account for the deviations in the received signal levels at the different frequencies from that predicted by the exponential model. So far, attempts to obtain the detailed characteristics from an ionosphere profile have been very limited due to the lack of experience in matching a theoretical model to the measured data. Intuition is extremely valuable in this matching process. If many attempts are required to obtain good fit, computer costs become very high.

A sample calculation using WAVEHOP to illustrate the character of the signal field strength as a function of distance in the range from 3 to 5 megameters for each of the 10 frequencies used in this measurement program is presented in Fig. 5(a), (b), and (c). The electron density profile used for these calculations is presented in the upper right corner of each figure. A rather steep electron gradient profile was chosen for these calculations to enhance the variability of the signals resulting from increased mode structure. The electron profile is, however, one that was found representative for some of the propagation data to be presented later. Each of the selectable parameters in the theoretical propagation model can have a significant influence on the nature of the propagated electric field. A limited number of examples will be presented to illustrate the influence upon the propagated signal of certain parameter changes.

Much discussion has taken place in recent years concerning the degree of influence on the propagated field of the earth's magnetic field. Figures 6(a) through 6(d) are plots of the field strength vs. distance for the isotropic case (that is, neglecting the effect of the earth's magnetic field) and the anisotropic case (that is, including the effect of the earth's magnetic field for both westward and eastward propagation). Plots at two frequencies, 10.9 kHz and 25 kHz, for two ionosphere conditions, $\beta = 0.5$ (-3 km) and $\beta = 0.3$, are presented to show the variability in the magnetic field effect at different frequencies and in the presence of different ionosphere parameters. The influence of th[illegible]gnetic field for this particular propagation path is more p[illegible] 0.9 kHz for both ionosphere profiles. The difference [illegible] for the signals propagating in different directions is [illegible] dB at the 4.2 megameter distance for both the $\beta = 0.3$ a[illegible] km) ionosphere. The influence of the earth's magnetic field on [illegible] propagation at 25 kHz, $\beta = 0.3$ ionosphere, would be difficult to measure, whereas the $\beta = 0.5$ (-3 km) ionosphere shows significant differences. It is noted from Fig. 6(d) that the signal relative minimum occurring at approximately 4 megameters is approximately 4 dB deeper for the eastward propagated signal than for the westward propagated signal and that the relative signal maximum just beyond 4.2 megameters is about 3 dB higher for the eastward propagated signal than for the westward propagating signal. It is also noted that the earth's magnetic field has negligible influence on the position of relative minima and maxima in the field strength vs. distance curves.

It is instructive to determine the relationships between variations in certain parts of the profile and the received signals in that such

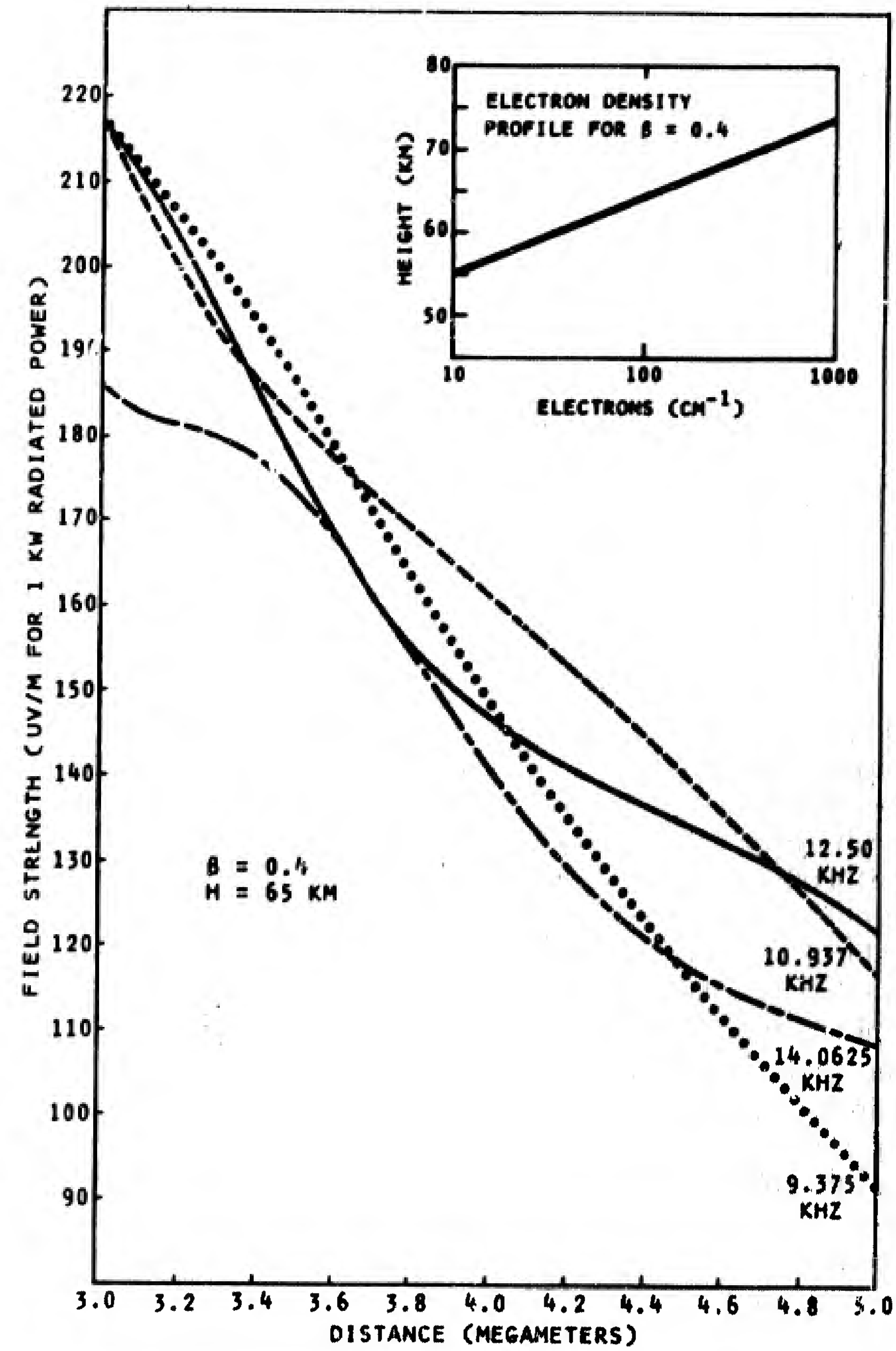

FIG. 5(a). Computed Signal Level vs. Frequency.

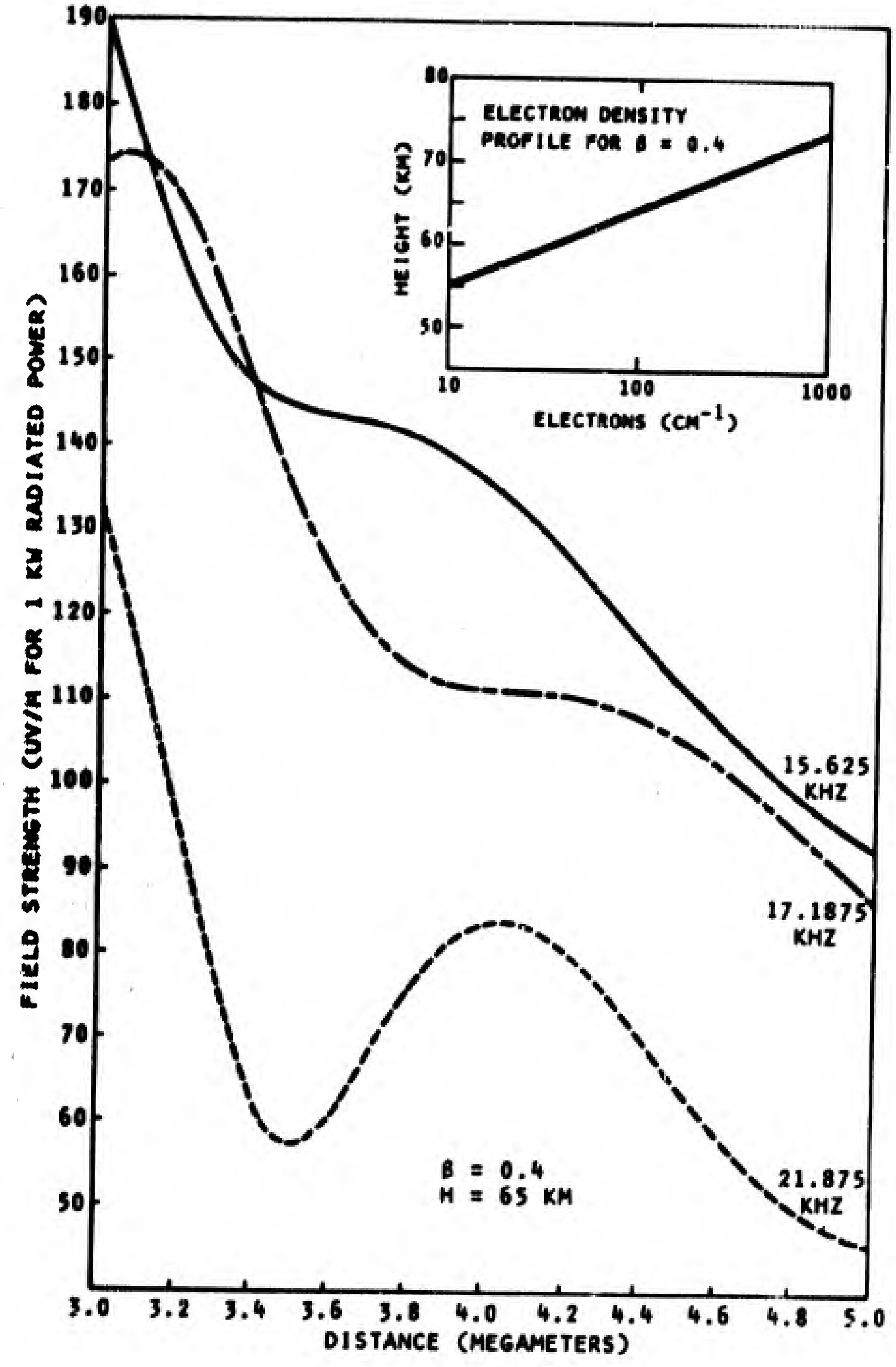

FIG. 5(b). Computed Signal Level vs. Frequency.

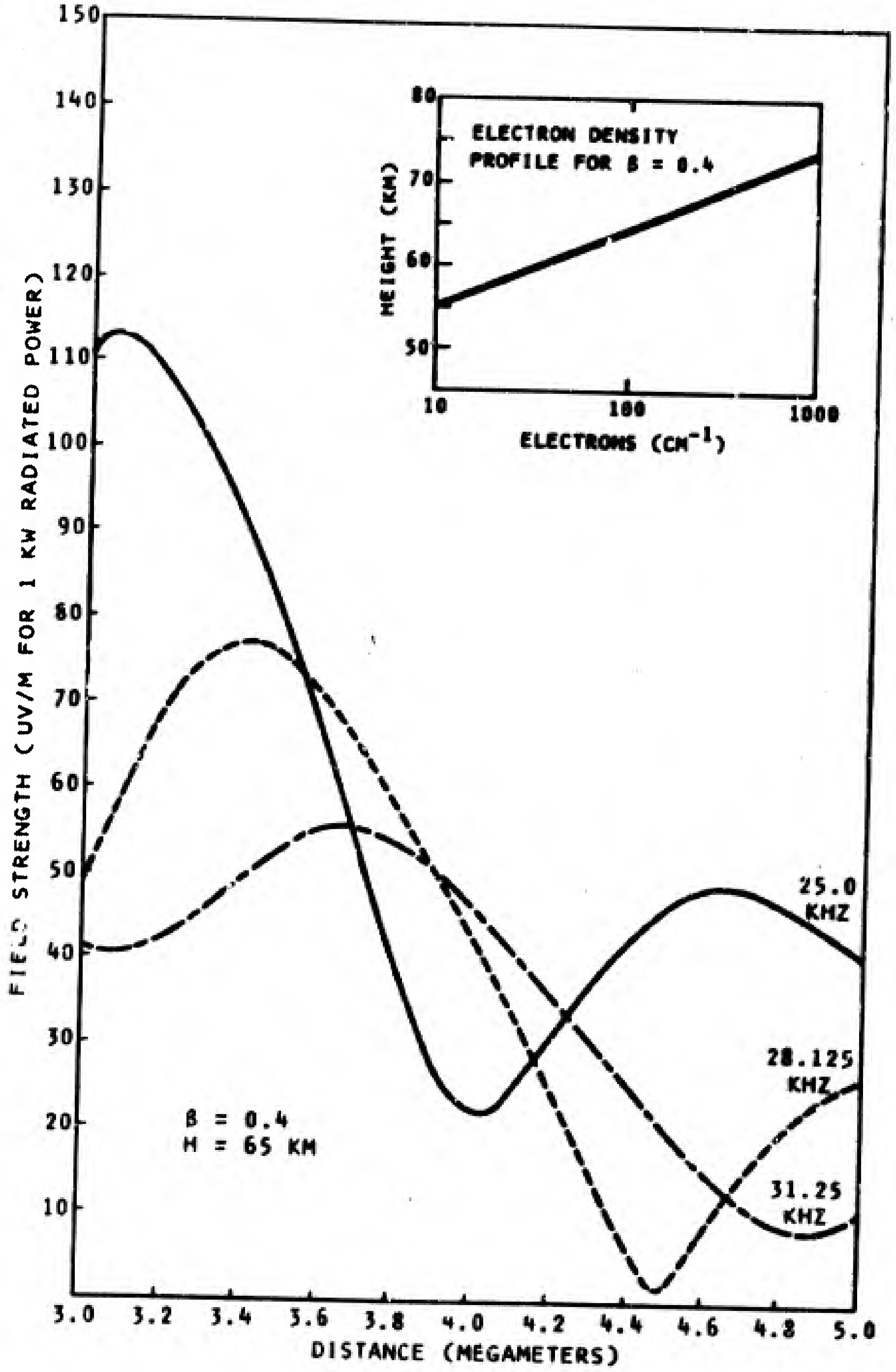

FIG. 5(c). Computed Signal Level vs. Frequency.

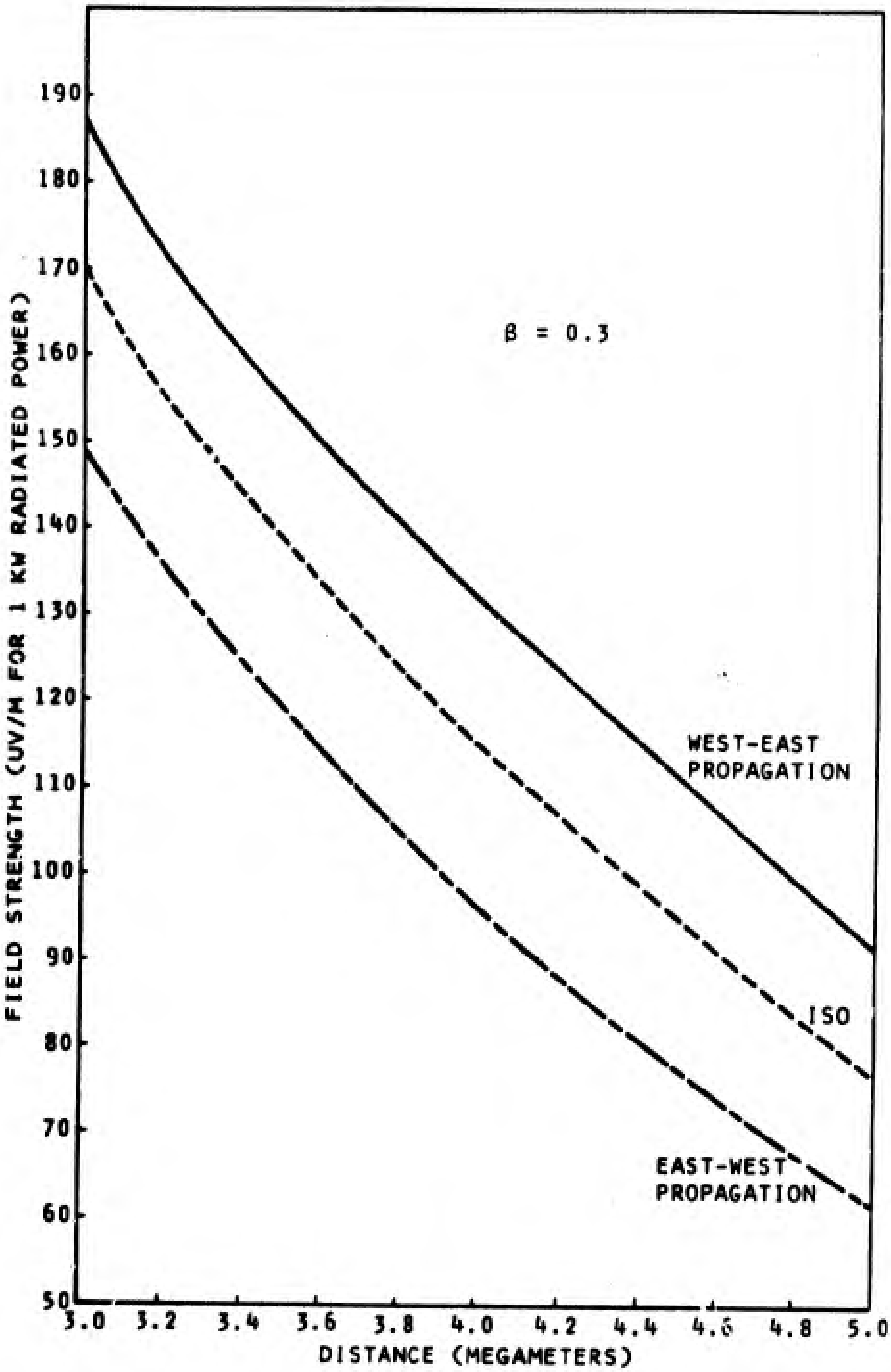

FIG. 6(a). Computed Field Strength vs. Distance for Isotropic and Anisotropic Cases (10.9375 kHz).

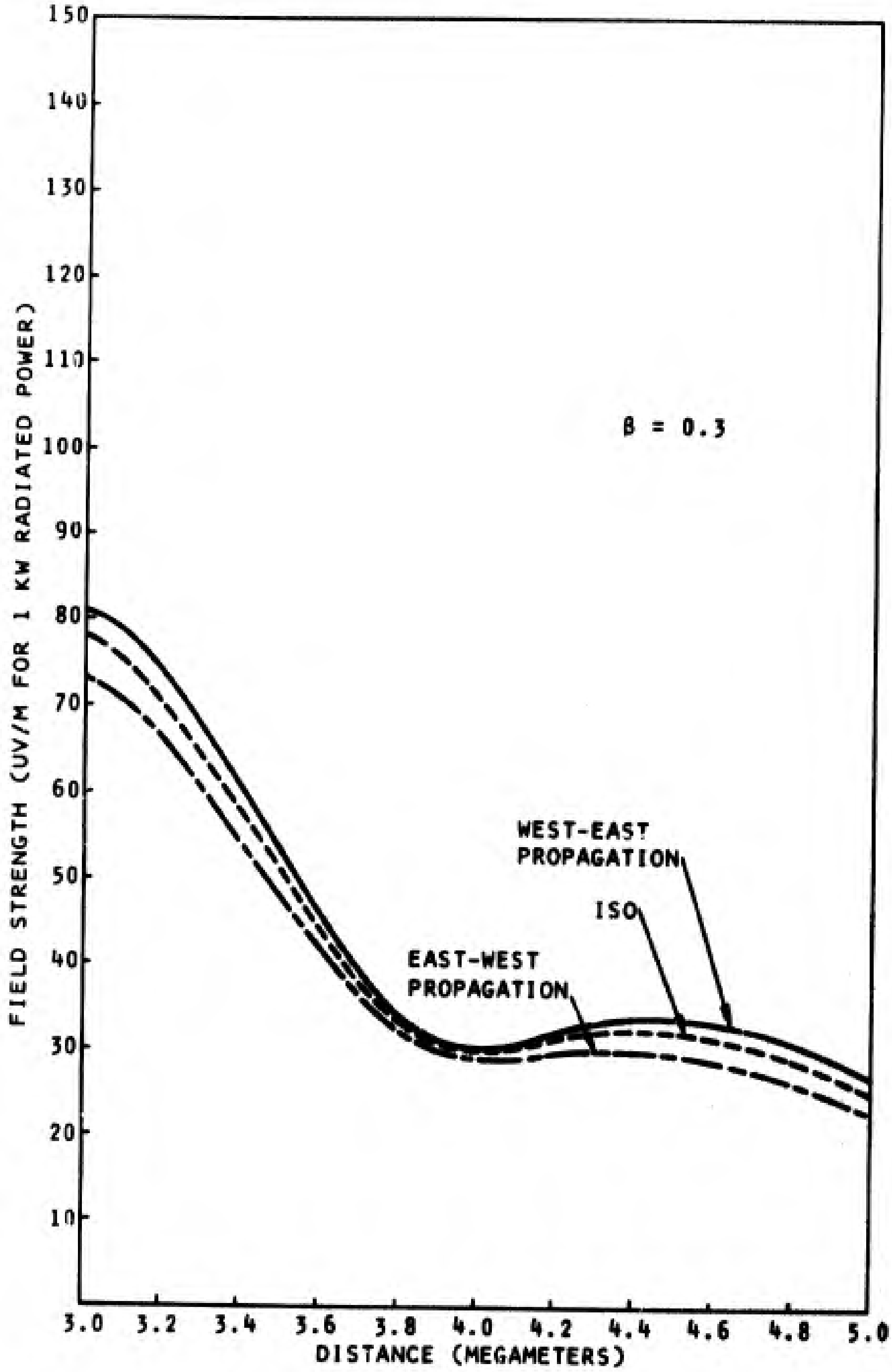

FIG. 6(b). Computed Field Strength vs. Distance for Isotropic and Anisotropic Cases (25 kHz).

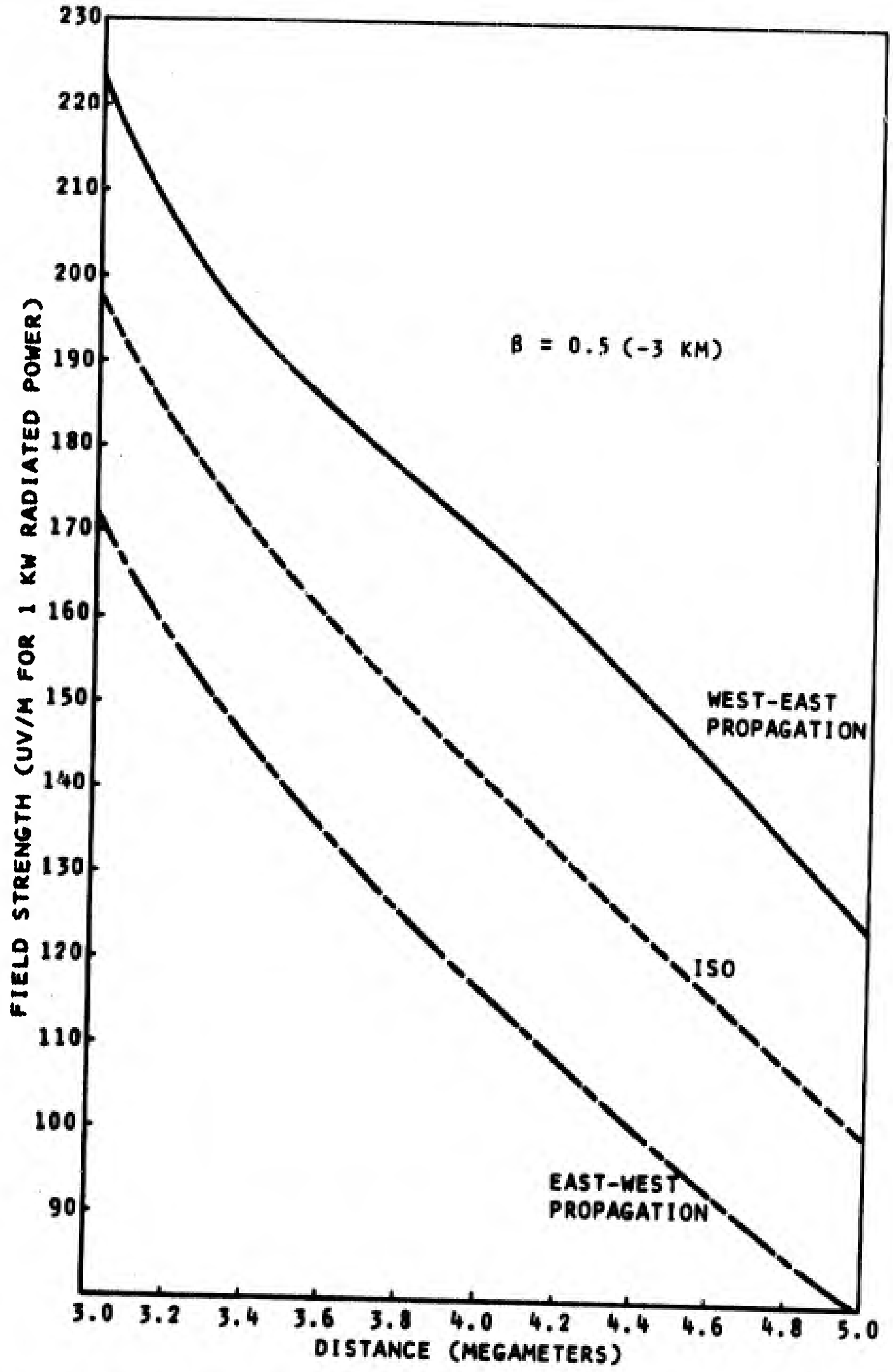

FIG. 6(c). Computed Field Strength vs. Distance for Isotropic and Anisotropic Cases (10.9375 kHz).

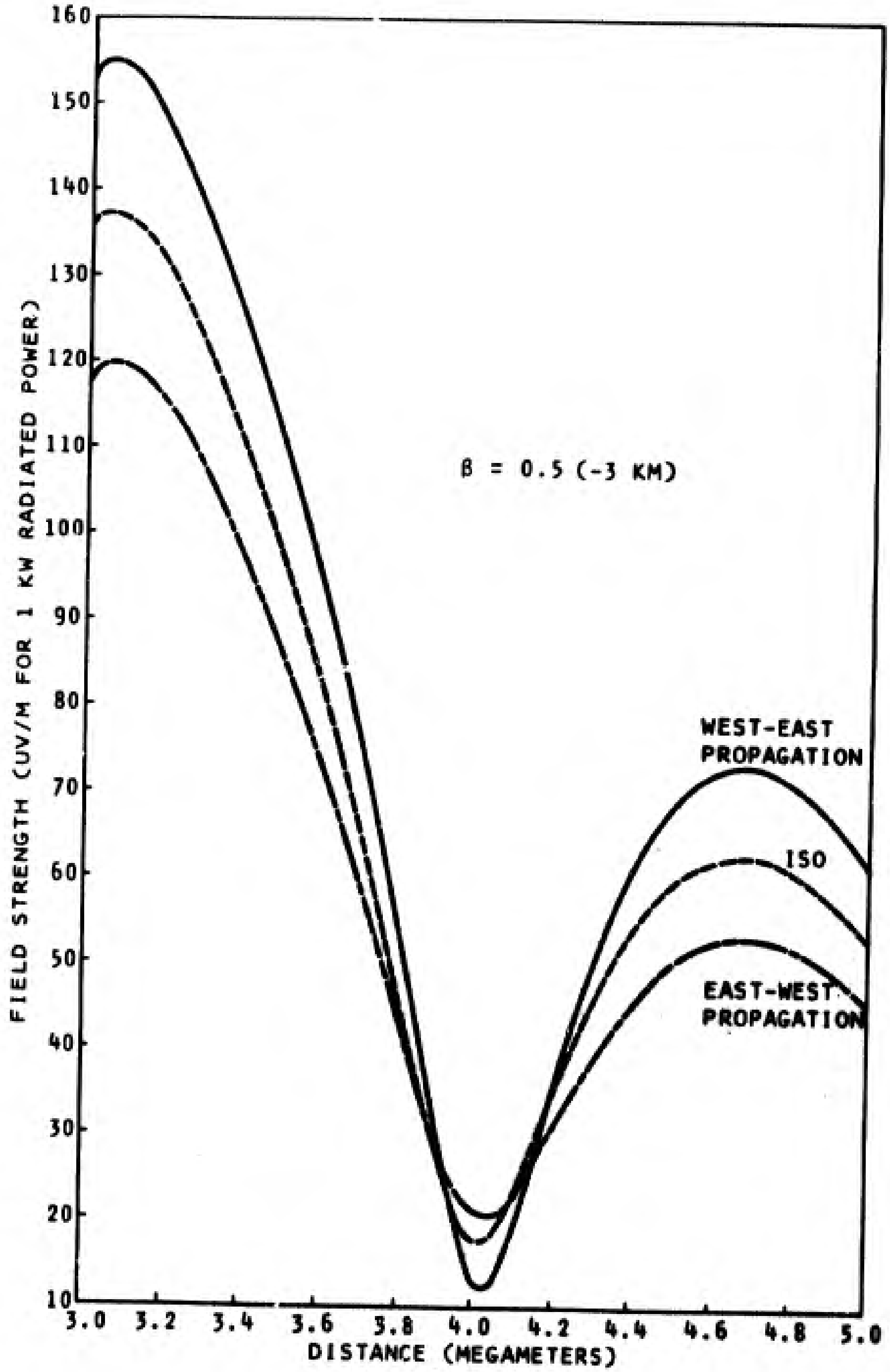

FIG. 6(d). Computed Field Strength vs. Distance for Isotropic and Anisotropic Cases (25 kHz).

information can be very valuable for determining the profile modifications needed for improving the agreement between theoretical calculations and measurement. A special significance can be attached to that part of a profile corresponding to the height which can be loosely referred to as the reflection height. This height is derived from Berry and Chrisman (Ref. 7) as the height at which the value of the transmission coefficient of the upgoing magnetic wave is reduced to 0.3 of its value at the bottom of the ionosphere. The electron density at this height is approximately 180 to 200 el/cm^3. The distances at which points of maximum constructive or destructive interference occur are very sensitive to the vertical height of reflection (200 el/cm^3). VLF propagation apparently becomes quite insensitive to the properties of the electron profile at densities above about 500 el/cm^3. This insensitivity is demonstrated by the curves labeled MOD A and B in Fig. 7(a) and (b). In these figures the computed field strength vs. distance is presented for the exponential profile and the modifications labeled A and B in Fig. 8 for the 9.375 kHz (Fig. 7(a)) and 25 kHz (Fig. 7(b)) frequencies. The exponential profile calculation was carried to an electron density value of 13,000 el/cm^3, whereas the calculations for modification A assumed that the profile decreased sharply to 1 el/cm^3 upon reaching a value of 1,000 el/cm^3. A similar calculation, but with the profile reduced abruptly to 1 el/cm^3 upon reaching 500 el/cm^3 was attempted, but the computer would not produce satisfactory results. The profile identified as modification B, which has a constant density with altitude of 500 el/cm^3 upon reaching this value, produced very minor changes in the computed fields. As an additional check the computer computations were stopped at the 500 el/cm^3 value and the results were compared with the reference exponential profile; no differences were observed. It is concluded from this series of calculations that profile data above the 500 el/cm^3 is not meaningful for propagation paths of this length either for predicting propagation conditions or for determining profile values from propagation measurements.

In contrast, the nature of the electron profile in the region below 100 el/cm^3 determines the effective reflection coefficient which is evidenced in both the general signal level and degree of mode structure. The curves in Fig. 7(a) and 7(b) labeled MOD C show the effect of increasing the electron density at low altitudes in the manner indicated in Fig. 8, MOD C. It is noted that the signal levels are generally lower than those for the exponential profile and that the mode structure is smaller. The curves in Fig. 7(a) and 7(b) marked MOD D show the results of decreasing the electron density at the bottom of the profile in the manner indicated by MOD D in Fig. 8. In this case the signal

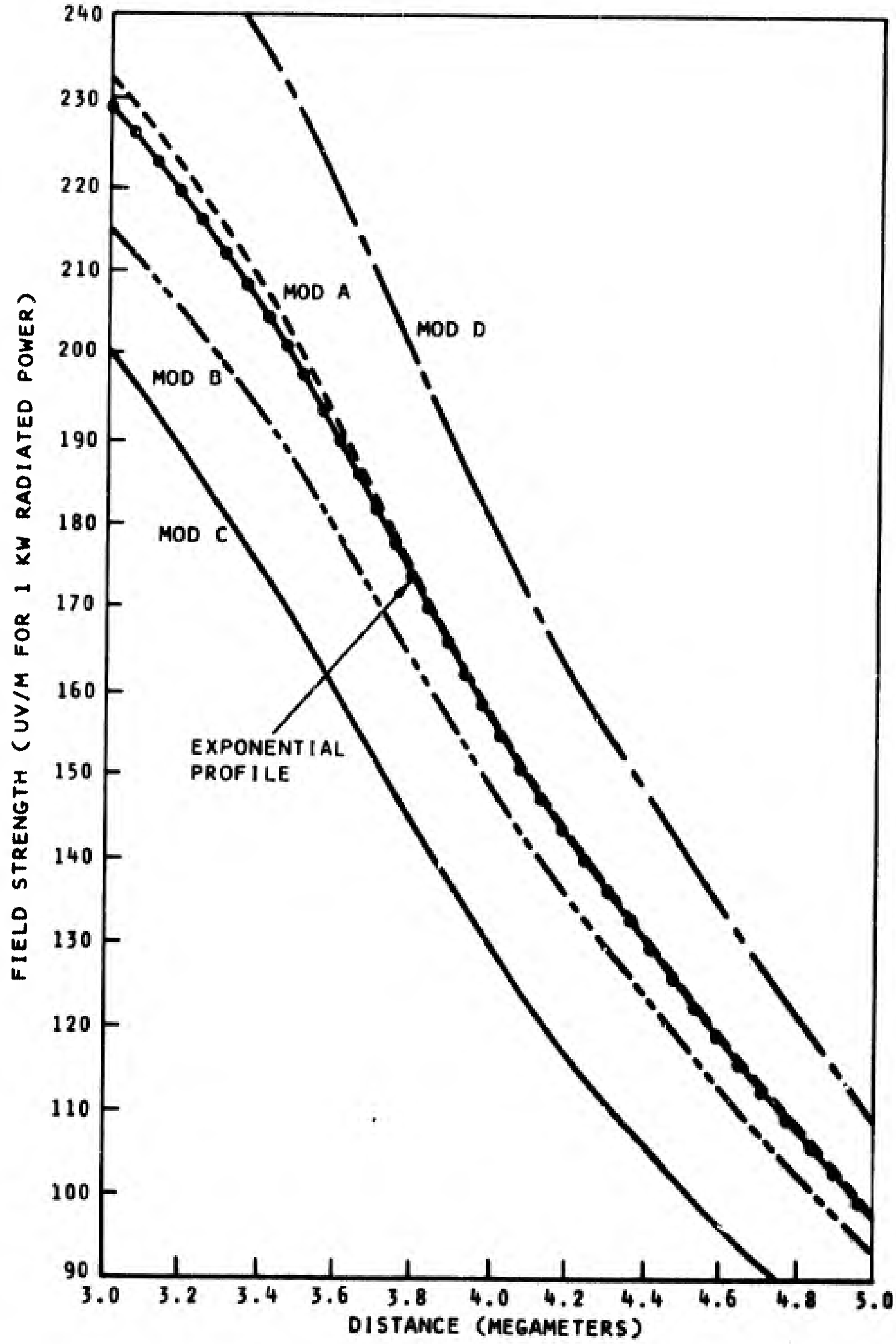

FIG. 7(a). Computed Field Strength vs. Distance for a Modified Electron Density Profile (9.375 kHz).

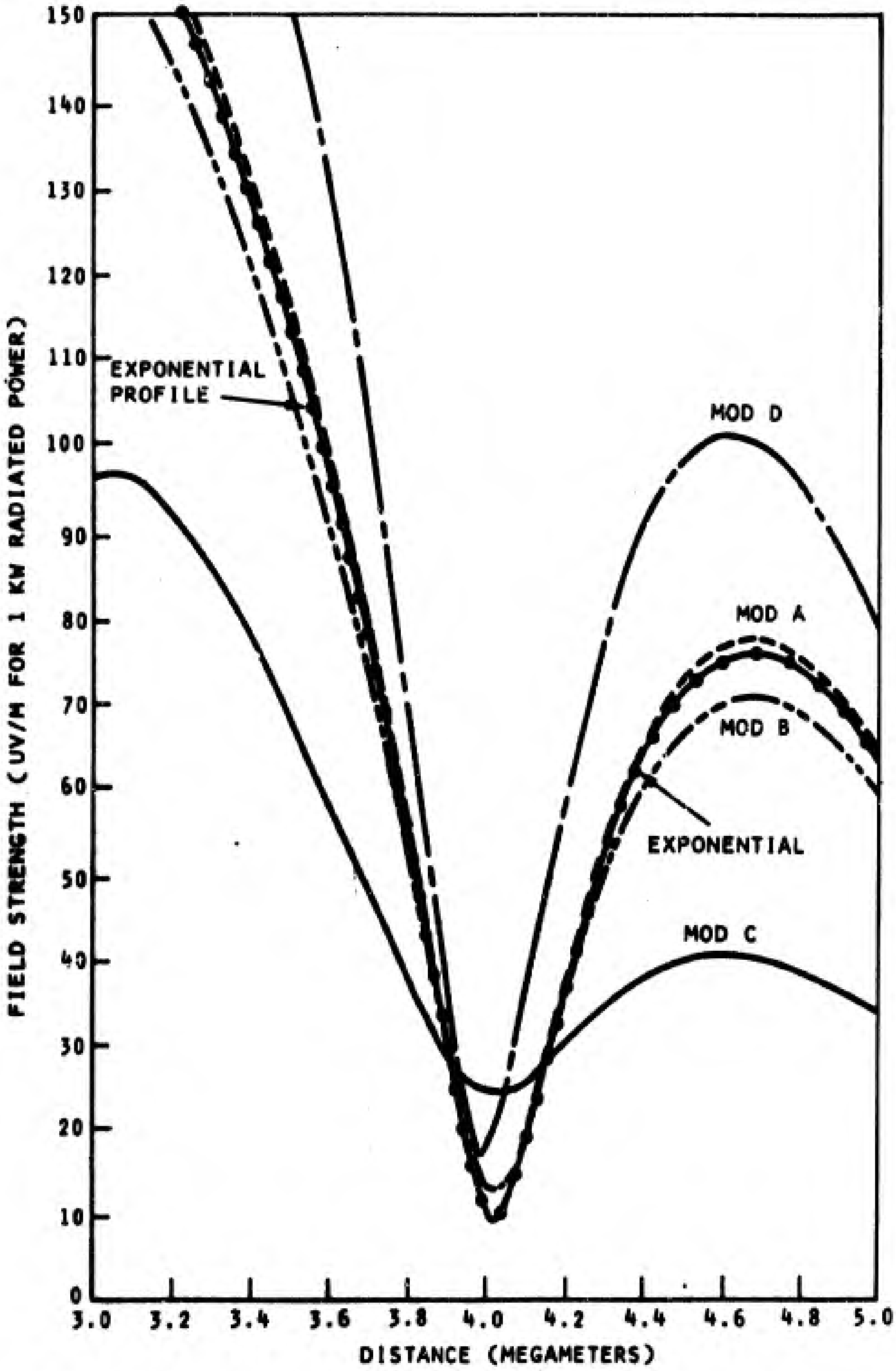

FIG. 7(b). Computed Field Strength vs. Distance for a Modified Electron Density Profile (25 kHz).

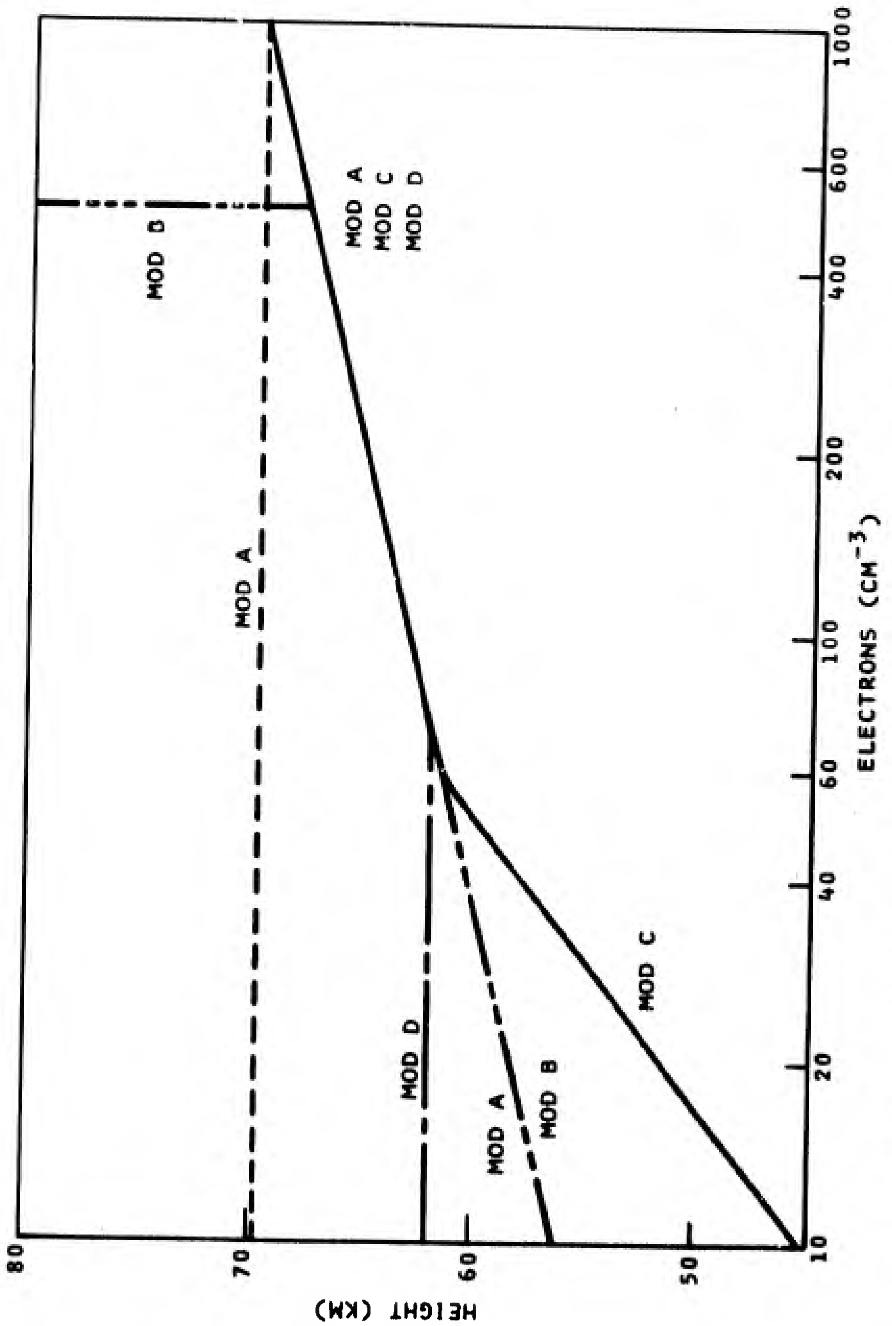

FIG. 8. Modified Ionospheric Electron Density Profiles.

levels are generally enhanced and the mode structure increased. It is noted that neither MODS C nor D produced a significant change in the distance at which the 25 kHz signal relative minima occur.

The computer solution of the reflection process in a region of low electron densities, such as the lowest part of a profile, becomes inefficient; that is, computing time becomes relatively long and computational accuracy diminishes. Because of this, it is of value to examine the influence of the portion of the profile with densities below 10 el/cm^3 on the computed fields. It was found that when the profile gradient equaled or exceeded $\beta = 0.4$, negligible differences were incurred in the results by neglecting the values below 10 el/cm^3. This was not the case for less steep gradients. When an attempt was made to compute the received fields with $\beta = 0.3$ exponential ionosphere down to an electron density of 1 el/cm^3, unsatisfactory results were obtained. For this reason, most of the profiles used in the current analysis were cut off at the lower end, at 10 el/cm^3. An assessment is now being made using the FULLWAVE program to determine if any serious effects are incurred.

As a final illustration, it is of value to determine whether the frequencies utilized in this sounder system provide the optimum information for determining the proper values for the propagation parameters. A computation is presented in Fig. 9 of the received field strength vs. frequency at the Southern California terminator of this path for two ionosphere profiles, $\beta = 0.3$ and $\beta = 0.5$ (-3 km). The X's placed on the $\beta = 0.5$ (-3 km) curve indicate the positions of the frequencies that were used for the March test series. The difference between the two curves is significant, particularly in the frequency range above 20 kHz. It is also evident that a better distribution of frequencies utilized in the sounder system could be made for this particular propagation path. The frequency 26.5 kHz indicated by the circled X has been added since March. The particular shape of the field strength vs. frequency curves is quite sensitive to the electron profile parameters; thus the determination of best frequency utilization cannot be based solely upon the data in this figure.

EXPERIMENTAL AND ANALYTICAL PROCEDURES

The heart of the correlation receiver used in the sounder system is a synchronous detector. The outputs of this synchronous detector are

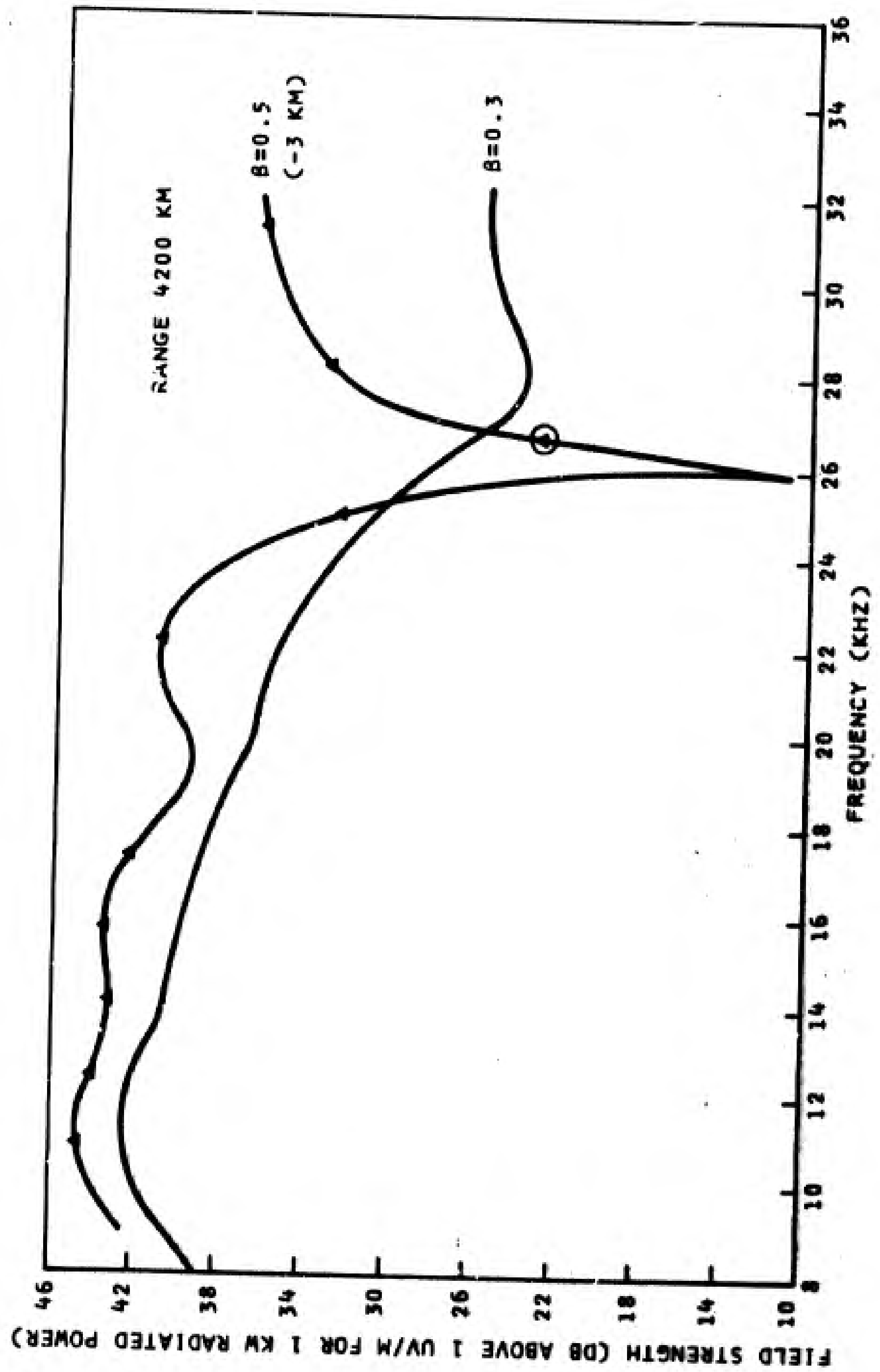

FIG. 9. Predicted Field Strength vs. Frequency.

the vector components X and Y of the received signal. The time-averaged outputs of the detected vector components are recorded both on strip chart records and on digital magnetic tape. A calibration signal is injected into the system at specific times during each test operation. The calibration method used (Ref. 11) consists of injecting a known signal current into a calibration loop placed parallel to one of the loops of the receiving antenna. The received calibration signal is recorded on the digital magnetic tape. Since a superdirective receiving array is normally used, the calibration of the signal loop must be converted to the response of the directive array. This is accomplished at the beginning of the VLF special transmissions by recording a period, typically 10 minutes, of the transmission with the single calibrated loop, and then switching to the directive array configuration and noting the differences in received signal level on each side of the switching time.

One of the major problems in system calibration is the determination of the actual radiated power from the transmitter. This is complicated by the fact that it has not been possible to precisely measure the radiation pattern of the transmitting antenna, and one must assume that the theoretical radiation pattern and its relationship to the measured ground wave off of the end of the antenna are valid. The transmitter radiated field has been measured by placing a VLF receiver 40 km from the transmitter along the path in the direction of California. This ground wave signal is also recorded on digital magnetic tape.

The calibration data from both the radiated field monitor and the receiver injection signal is utilized in the computer processing of the data to provide a data output or display in terms of the equivalent received field strength and phase vs. time for a radiated power of 1 kW as presented in Fig. 10. Values of interest at specific times can easily be tabulated automatically from the computer processing or can be read from the computer processed records.

The data analysis is typically conducted in the following manner. Experimental data on field strength vs. frequency is acquired for a specific time of interest. A calculation from the theoretical model using logical propagation parameters for the specific time of interest is also obtained. A comparison is then made between the observed and computed field strengths. The discrepancies between the experimental and computed data then provide guidance for a new estimate of propagation parameters. Additional computations are made until a satisfactory match is obtained between the experimental data and the

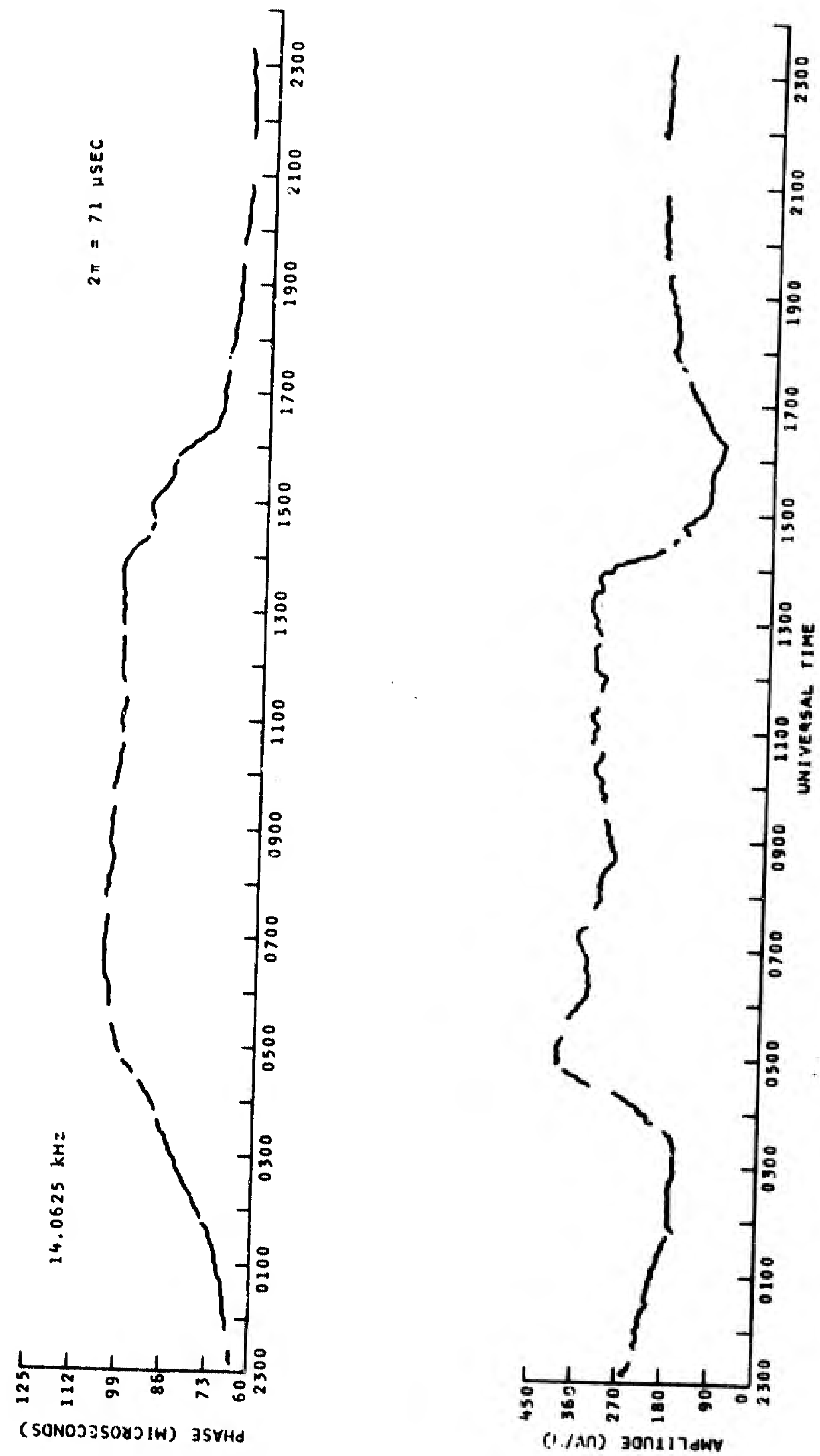

FIG. 10. Equivalent Received Field Strength and Phase vs. Time for a 24-hr Period on 13-14 March 1967 (14.0625 kHz).

propagation model. To illustrate this procedure, the predicted field strength at the 4.166 megameter distance for each of the 10 sounder frequencies is presented in Fig. 11 for four different electron density profiles. In this figure, the experimental data for midpath noon on 7 March 1967 which has been normalized to the 9.375 kHz computed value for each of the profile models is compared with the computed values for each of the profiles. The lines connecting the noted values are for identification and pattern recognition only as the field between points may vary in a significantly different manner as evidenced by Fig. 9. It can be seen from Fig. 11 how the shape of a curve through the predicted values changes with different ionosphere characteristics. The essential features of the curve appear to be the general slope between the 9.375 kHz and 21.875 kHz frequencies, and the relative positions of the field strength values for the three highest frequencies. The relative positions of the three highest frequencies are very sensitive to the height of the profile. That is, if a given profile shape is adjusted in height, the relative positions of the field strength values for the three highest frequencies will change significantly. This has been illustrated with the electron profile models indicated as β = 0.4 and Deeks. In this figure, the predicted field strengths are also shown for the β = 0.4 ionosphere lowered 2 km and for the Deeks ionosphere raised 3 km. The general slope of the curve from the lowest frequency to 21.8 kHz appears to be most sensitive to the steepness of the electron gradient from 0 to 200 el/cm^3. The values of the higher frequencies, while quite sensitive to the height of the profile in the region near 200 el/cm^3, are also strongly affected by the absorption produced by the lower density portion of the profile. Other fine structure on the shape of the field strength curves is probably primarily due to minor variations in the electron density profile.

The electron density profiles used for the models represented in Fig. 11 are presented in Fig. 12. The ionospheres indicated by β = 0.3, β = 0.4, and β = 0.5 are after the notation of Wait (Ref. 9). In this notation the exponential electron density and collision frequency profiles are:

$$N(Z) = N_o \exp\left[b(Z - h')\right]$$

$$\nu(Z) = \nu_o \exp\left[-a(Z - h')\right]$$

$$N_o = 3.93 \times 10^8 \ \frac{\text{electrons}}{m^3}$$

$$\nu_o = 5 \times 10^6 \ \text{sec}^{-1}$$

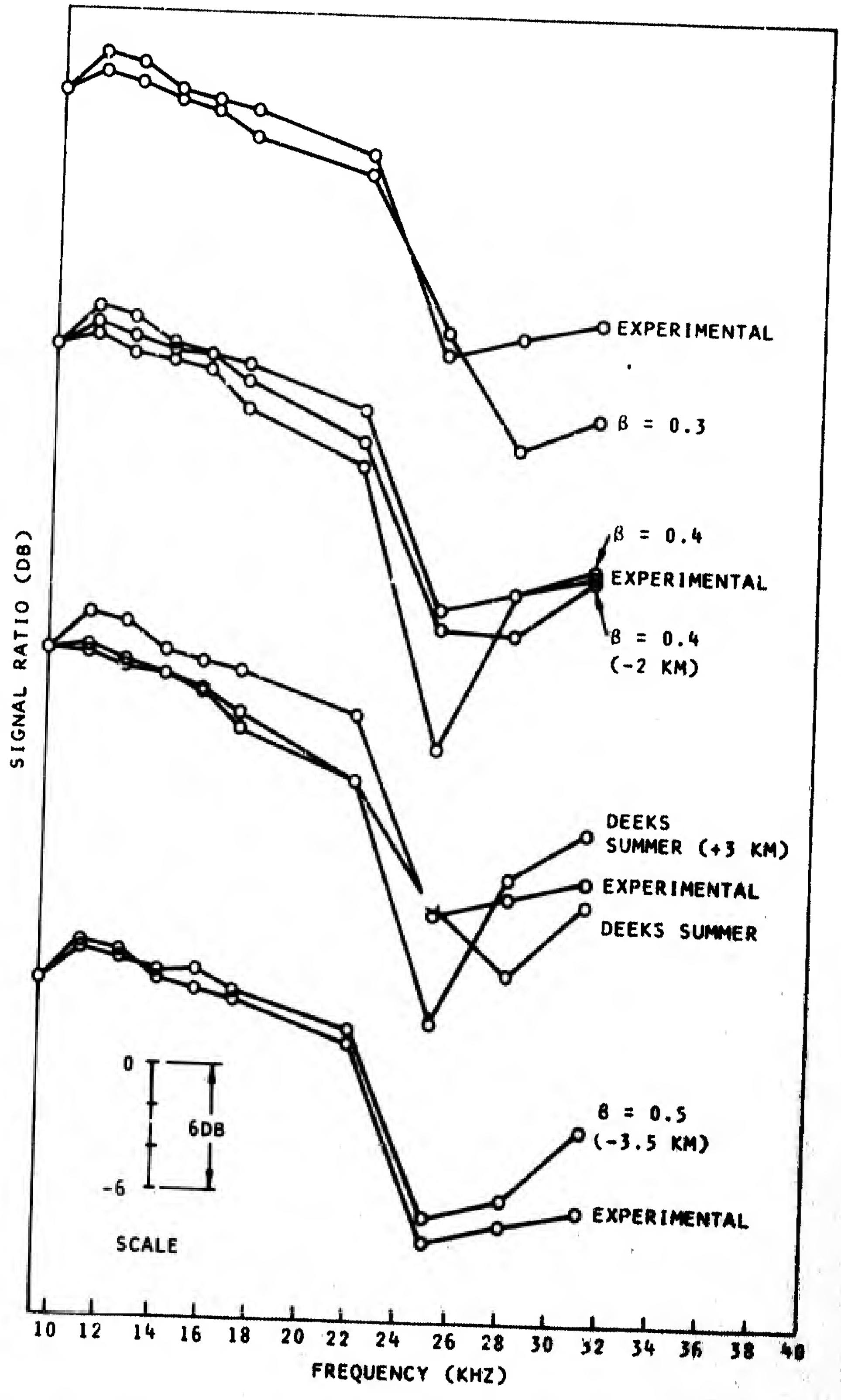

FIG. 11. Normalized Predicted and Measured Field Strength.

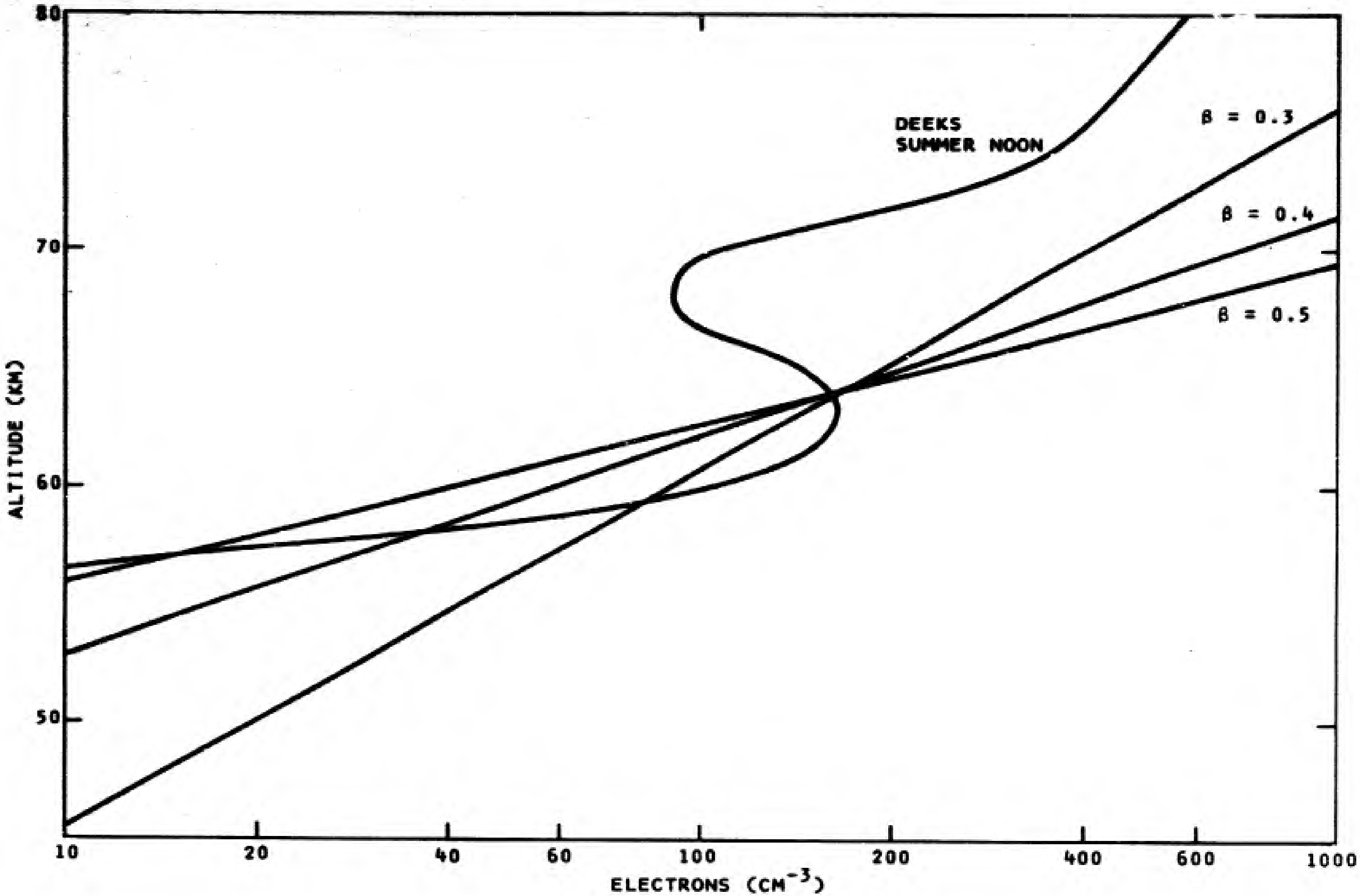

FIG. 12. Electron Density Profiles.

$h' = 70$ km

$a = 0.15$ km^{-1}

These exponential profiles are identified by the parameter $\beta = a + b$.

A table of electron density (N(Z)) as a function of height (Z) may be determined from the above equations as

$$N(Z) = 3.93 \times 10^{+8} \exp \left[(\beta - 0.15)(Z - 70)\right]$$

For this report such profiles were determined for $\beta = 0.3$, $\beta = 0.4$, and $\beta = 0.5$. These profiles were adjusted in height to obtain the best comparison with the data. The best fit for all profiles, Fig. 12, was obtained when the electron density of 200 el/cm^3 occurred at 65 km. In accordance with the above definition, these profiles have a value of β slightly different than indicated, because of this height adjustment. The electron profiles have the same gradient, however. The profile labeled Deeks was found to be representative of summer noon conditions over England at sunspot minimum (Ref. 10).

It has been found that the position of the field strength values for the four highest frequencies is a very sensitive indicator of the actual "reflection height" for any given profile configuration. As stated earlier, for the particular computation illustrated in Fig. 11, it was found that the best fit to the experimental values for any assumed profile model was obtained when the value of 200 el/cm^3 was placed very close to 65 km height. This high sensitivity of the upper frequencies to profile height results from the high mode structure existing. To illustrate this, the field strength vs. distance for two frequencies, 25 kHz and 28.13 kHz, is presented in Fig. 13 for both the Deeks profile and the Deeks profile raised 3 km. It is noted from this figure that as the ionosphere height is raised, the 25 kHz signal at the 4.166 megameter distance decreases, whereas the 28.13 kHz increases, both by a significant amount. Also, the positions of relative signal minima for each of the two frequencies move to greater distances as the ionosphere height is raised. A first approximation useful for profile matching is that the position of the signal minima will increase in distance almost 100 km for each kilometer increase in profile height. It has been found that with care one can generally determine the "profile height" within 1/2 km.

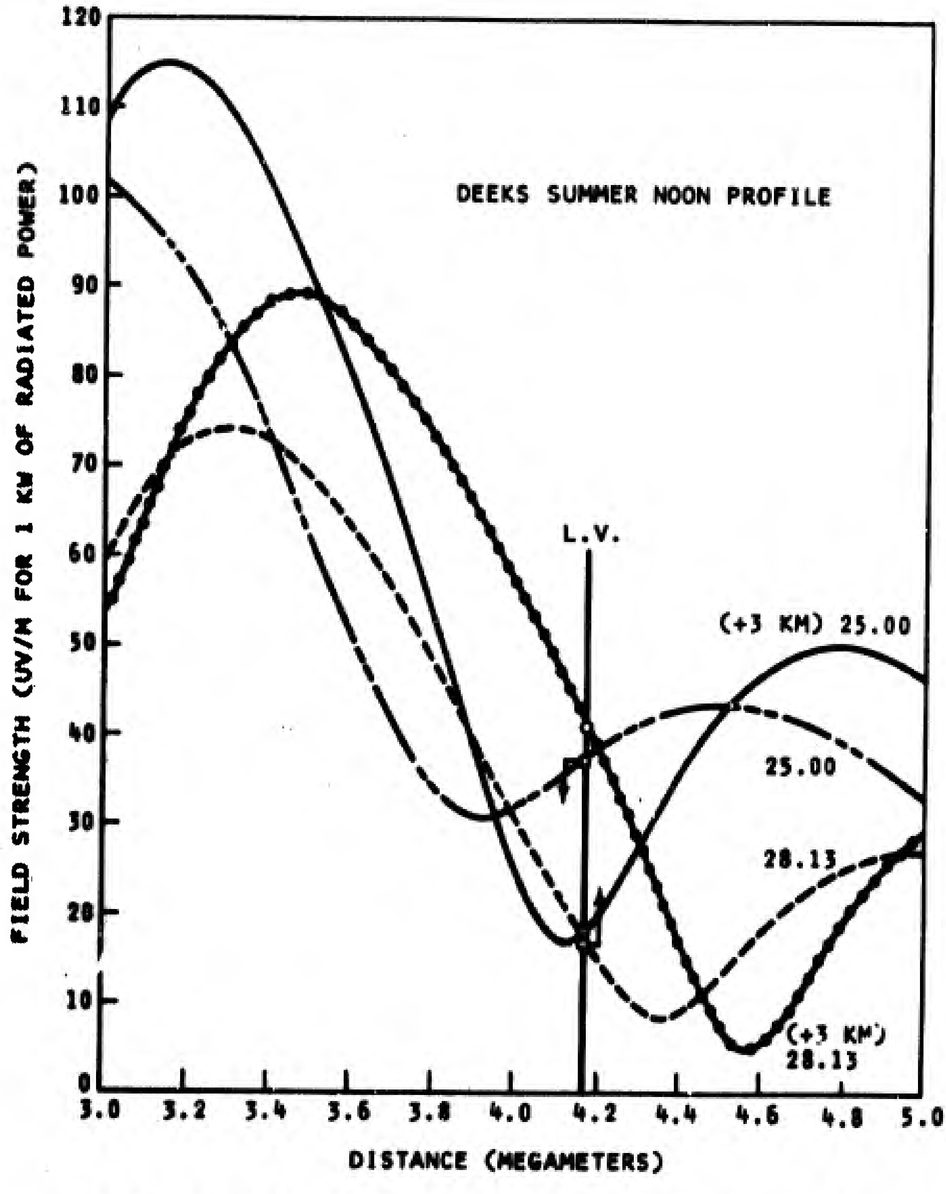

FIG. 13. Field Strength Variation for Change of Ionosphere Height.

EVALUATION RESULTS

The objective of this investigation was to determine propagation parameters for the March equinox period. Within the confines of the available data, this included deriving the best fit electron profiles for specific conditions, assessing the repeatability of propagation conditions for similar periods such as midpath noon on different days, and determining the variability of the profile with changes in geophysical conditions such as solar zenith angle or solar activity. Fortunately, during this period solar activity varied greatly.

The midpath noon time was selected as that most likely to provide the greatest uniformity of propagation conditions along the path. The values of the received field strengths for each of the 10 frequencies recorded at the midpath noon on the dates of 3, 6, 7, 13, and 14 March are presented in Fig. 14. The best fit profiles derived for the dates of 3, 7, and 14 March are presented in Fig. 15. Attention is directed to the profile derived for each of these dates in relationship to the level of the solar 10.7 cm radio flux recorded for these dates presented in Fig. 16. Clearly, there is a consistent relationship between the solar radiation level and the profiles presented in Fig. 15. The solar flux values plotted in Fig. 16 are the local noon daily averages for the undisturbed sun as recorded at Corona, California. These recorded values are compared with the daily values reported from Ottawa (Ref. 12). Recently, evidence has been acquired (Ref. 13) to indicate that short-wavelength x-rays produce significant ionization within the D region during periods of high solar activity (that is, periods of activity other than that associated with solar flares). An empirical relationship has been established (Ref. 14) between the short-wavelength x-ray flux level and the 2800-MHz radio noise intensity. The 2800-MHz radio flux Φ has been reported to be related to the x-ray flux J as follows:

$$J_{(2\text{-}8A)} = 1.4 \times 10^{-5} (\Phi_{2800} - 73) \text{ in ergs cm}^{-2} \text{sec}^{-1}$$

Comparison of satellite x-ray flux measurements obtained from an NRL satellite (Ref. 15) with 2800-MHz flux data acquired at the Corona Laboratories would indicate that this relationship is not very exact. This is illustrated in Fig. 17. Unfortunately, x-ray data was not available from the NRL satellite for the month of March 1966; this is the reason for utilizing the radio flux data. Referring to Fig. 16, the dates for which propagation data were collected are indicated along the bottom

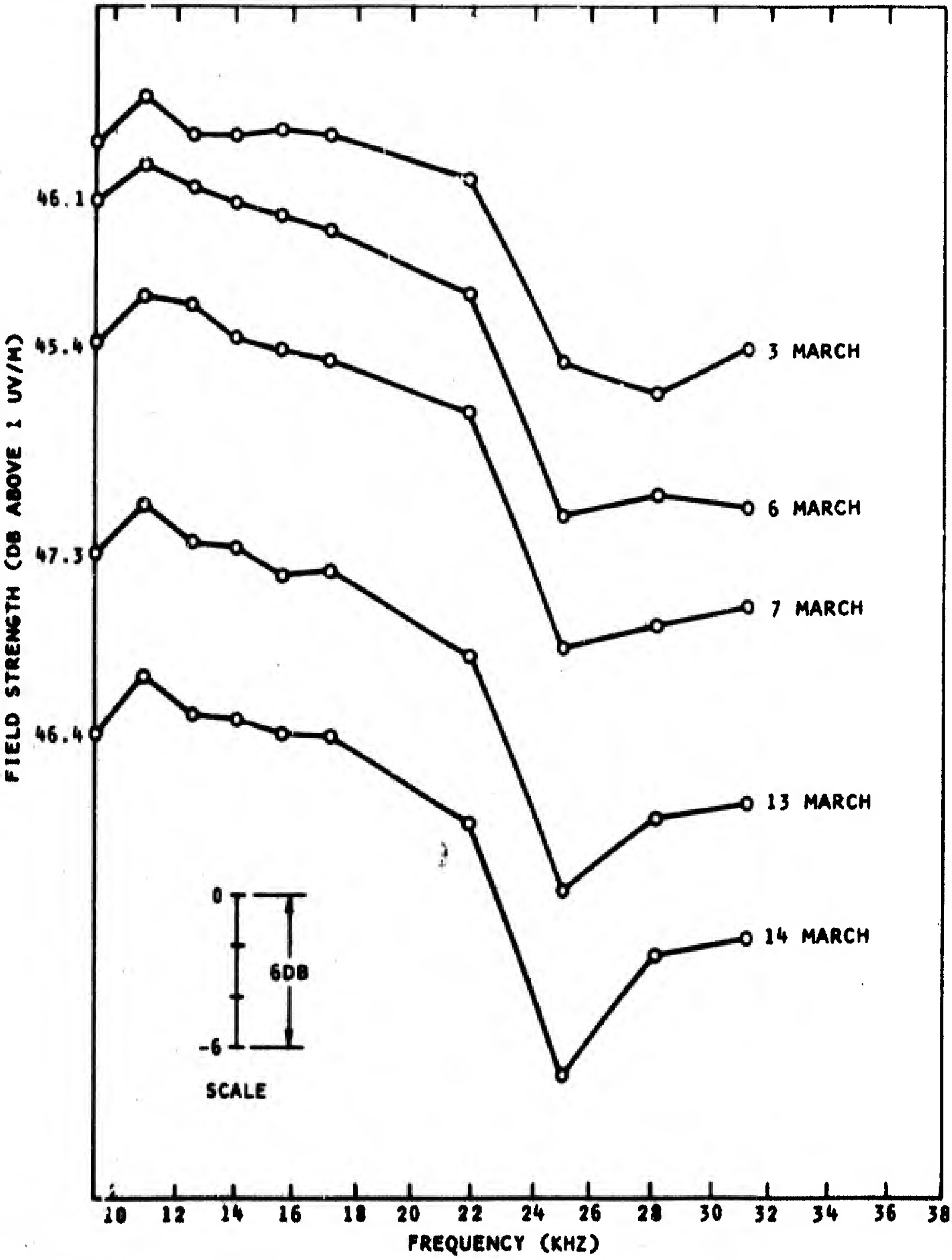

FIG. 14. Experimental Values for Field Strength vs. Frequency at Midpath Noon (2200 U.T.) during March 1967.

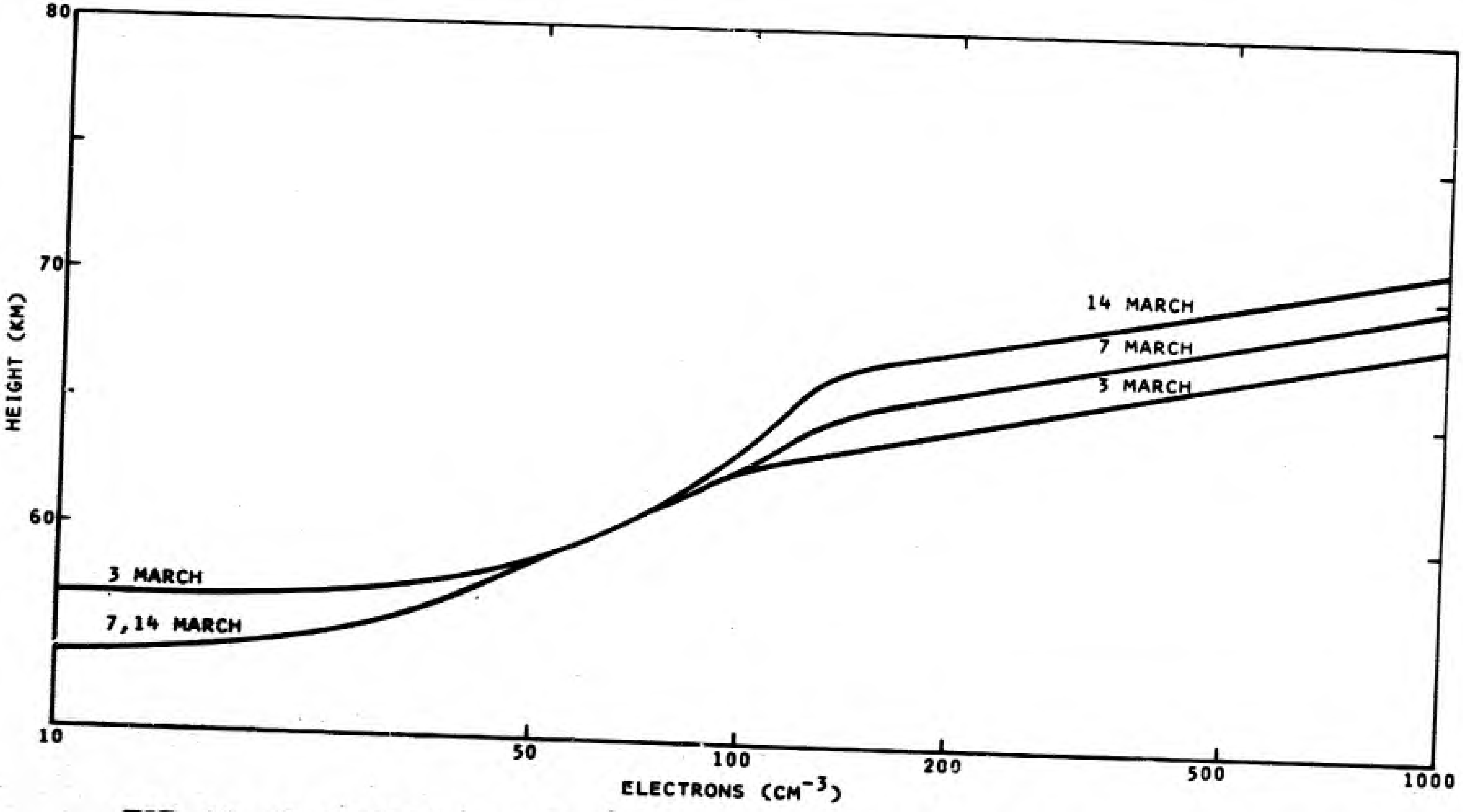

FIG. 15. Best-Fit Electron Density Profiles for March 1967 Experimental Data at Midpath Noon (2200 U.T.).

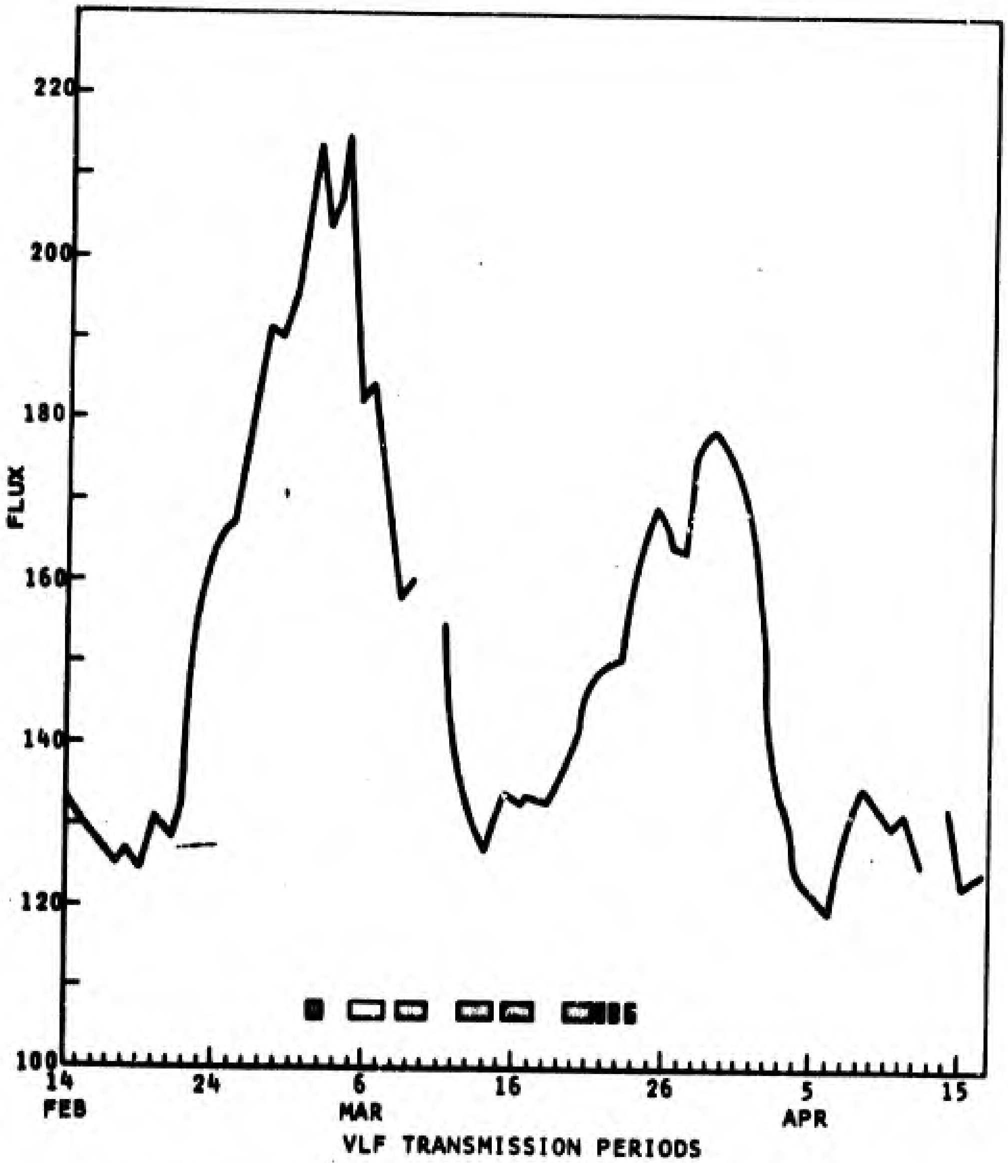

FIG. 16. Solar Radio Flux for February, March, and April 1967.

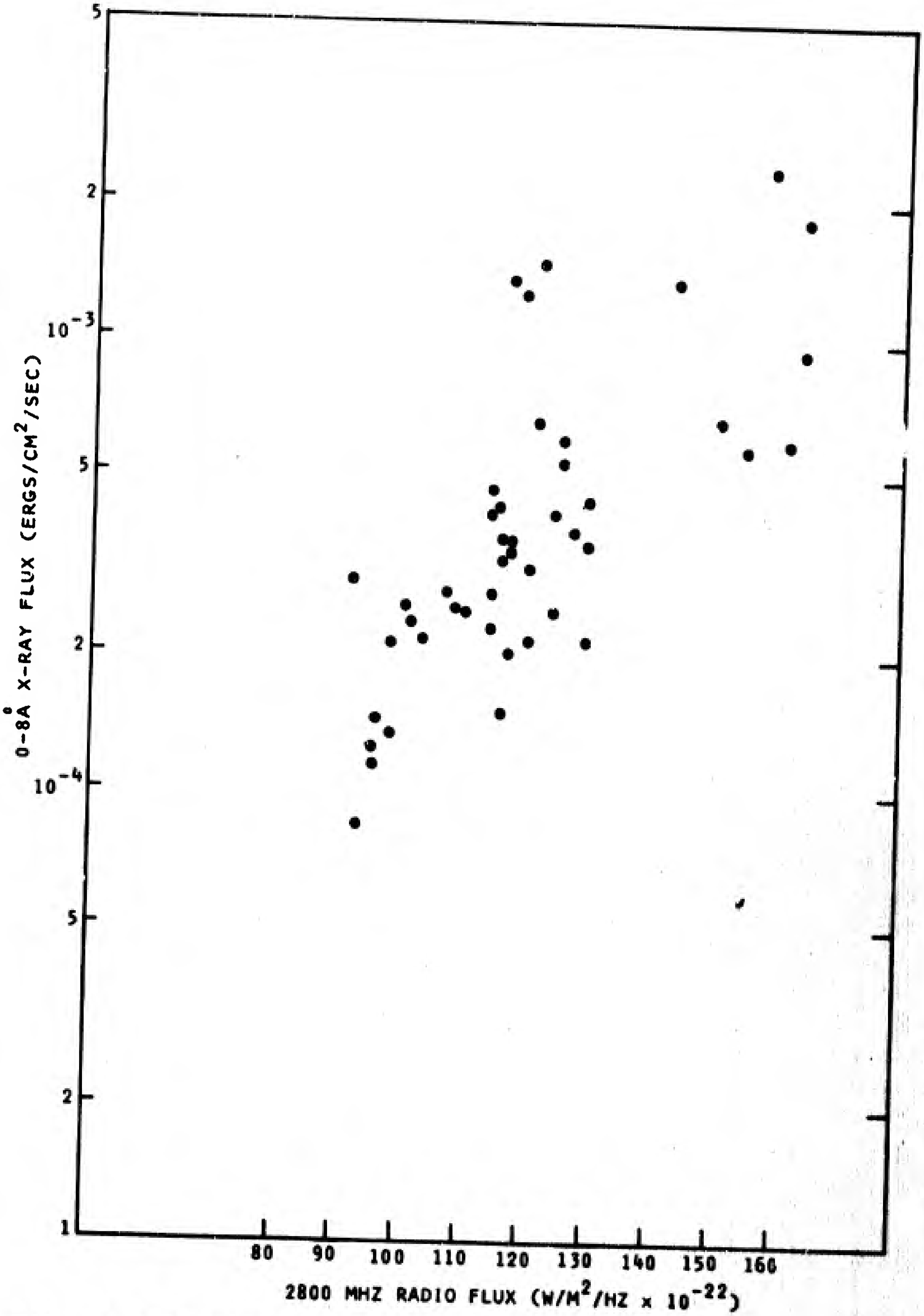

FIG. 17. 0-8 A X-Ray Flux vs. 2800 MHz Radio Flux for Period Between 1 November 1966 and 15 December 1966.

of the graph. It is further noted that even for 14 March, when the solar radiation level was at its relative minimum, the profile had a steeper electron gradient than that of $\beta = 0.3$, which is frequently used to describe daytime propagation.

In a similar manner the time variability of propagation parameters has been examined; because of the manner in which the propagation measurements were scheduled, the evaluation was broken up into two categories, that for the time period from sunrise till midpath noon and that from the midpath noon until sunset. The measured received field strengths for the transmission period from sunrise until noon for the 7 and 14 March dates are presented in Fig. 18 and 19. Likewise, the measured field strengths for each of the 10 frequencies for the period from noon until sunset on the path for the dates 6 and 13 March are presented in Fig. 20 and 21. The time variability of the received field strength at the higher frequencies which was described in the discussion of the data presented in Fig. 3(a), (b), and (c) is quite pronounced in the plots presented in the last four figures.

Additional insight into the characteristic behavior of the signals can be gained from a measure of the relative phase changes occurring over the time intervals of interest. This is particularly true for those periods of time when ionosphere changes produce only minor variations in signal absorption or mode structure, such as during the midday period. Neither a measure of received absolute phase nor relative phase between frequencies can be derived from the measurements. Because of this the change in phase with time for each frequency relative to a reference time, in this case midpath noon, has been chosen as a measurement parameter. Plots of received phase in degrees vs. signal level in dB, with noon phase values equated to zero, are presented in Fig. 22 through 25 for, respectively, the sunrise to noon and noon to sunset periods of 7, 14, 6 and 13 March. The times for each of the data values correspond to the appropriate times for each of the curves in Fig. 18 through 21. It is to be emphasized that the complete path is in daylight during the time intervals represented. The illumination efficiency does vary significantly, however, as may be seen from the plots of solar zenith angle vs. time presented in Fig. 26.

Some progress has been made in determining the electron profile variation that occurs over the corresponding time intervals, but completely satisfactory results have not been obtained to date. It is necessary, because of measurement limitations, to derive an initial or reference profile using only the field strength data. The success in

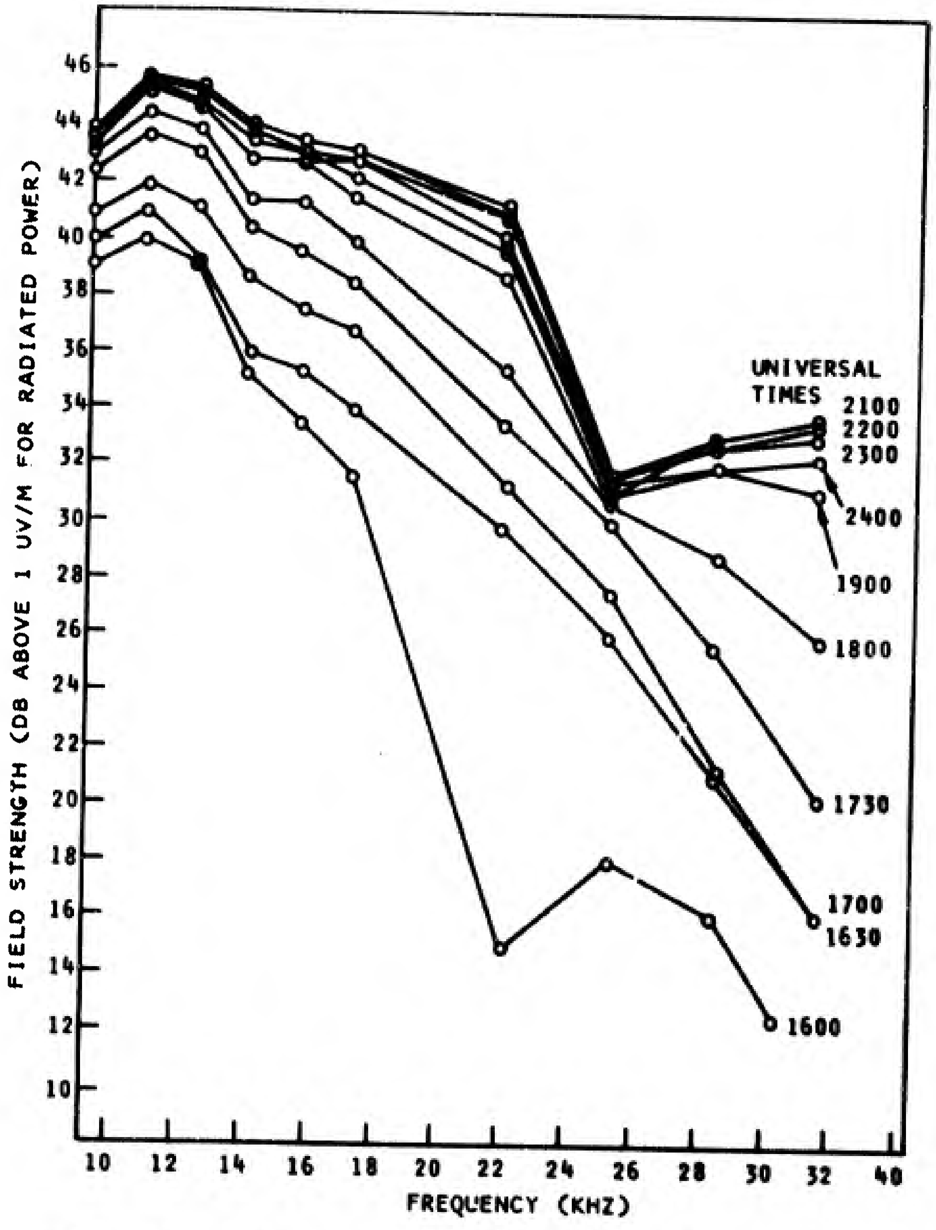

FIG. 18. Experimental Values of Field Strength vs. Frequency from Sunrise to Noon on 7 March 1967.

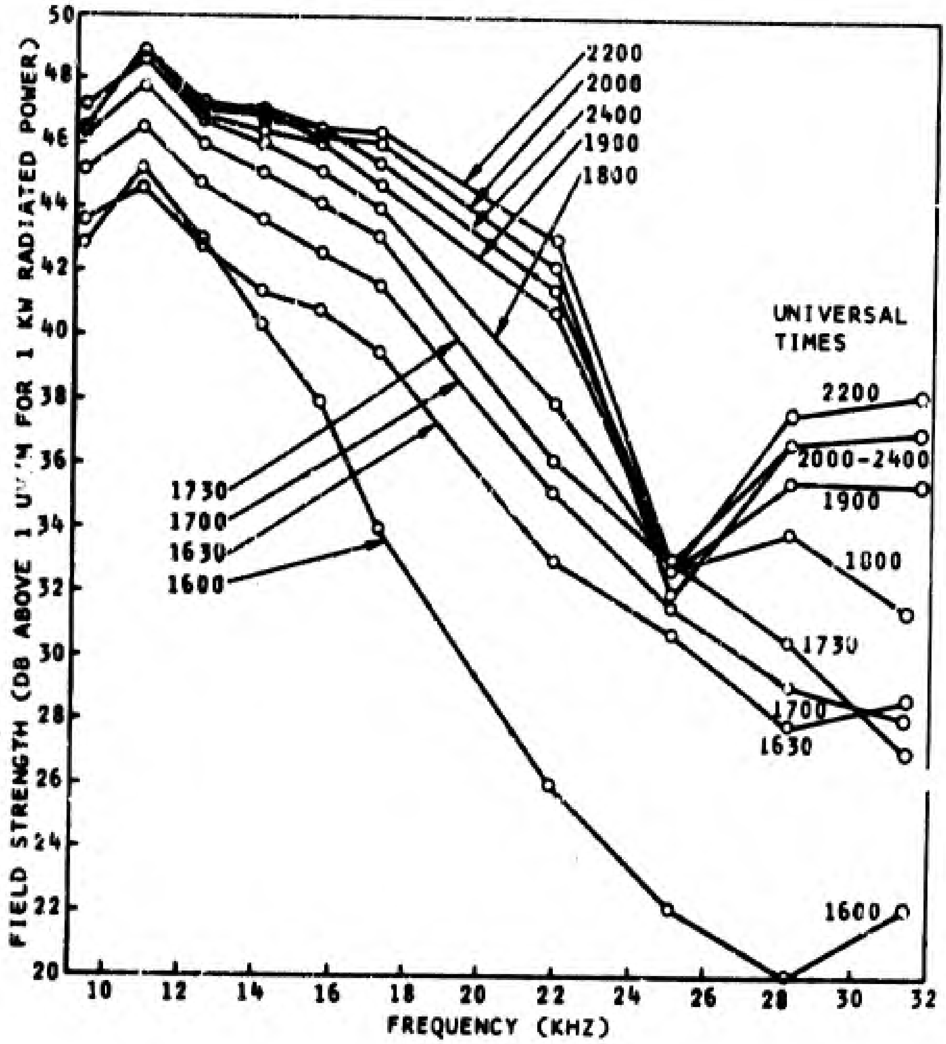

FIG. 19. Experimental Values of Field Strength vs. Frequency from Sunrise to Noon on 14 March 1967.

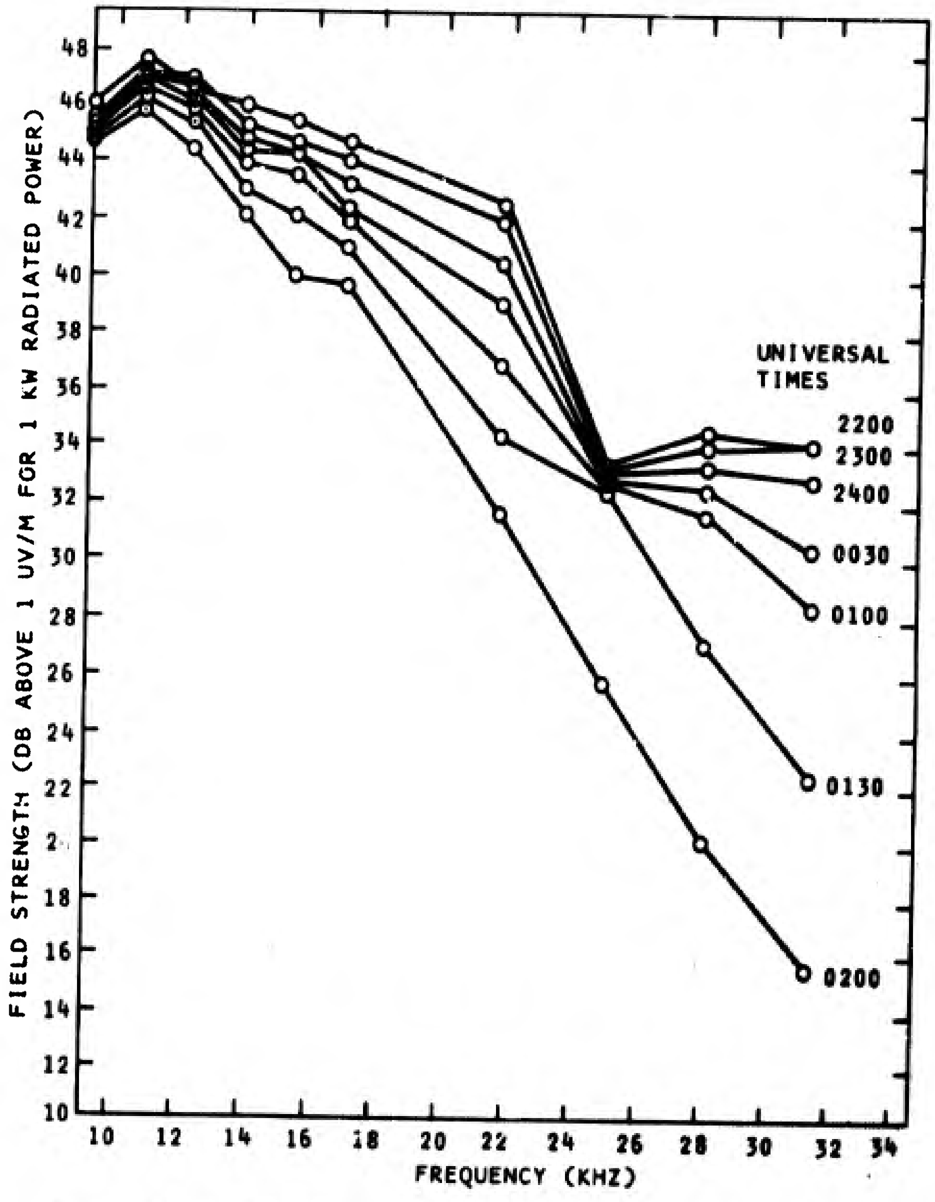

FIG. 20. Experimental Values of Field Strength vs. Frequency from Noon to Sunset on 6 March 1967.

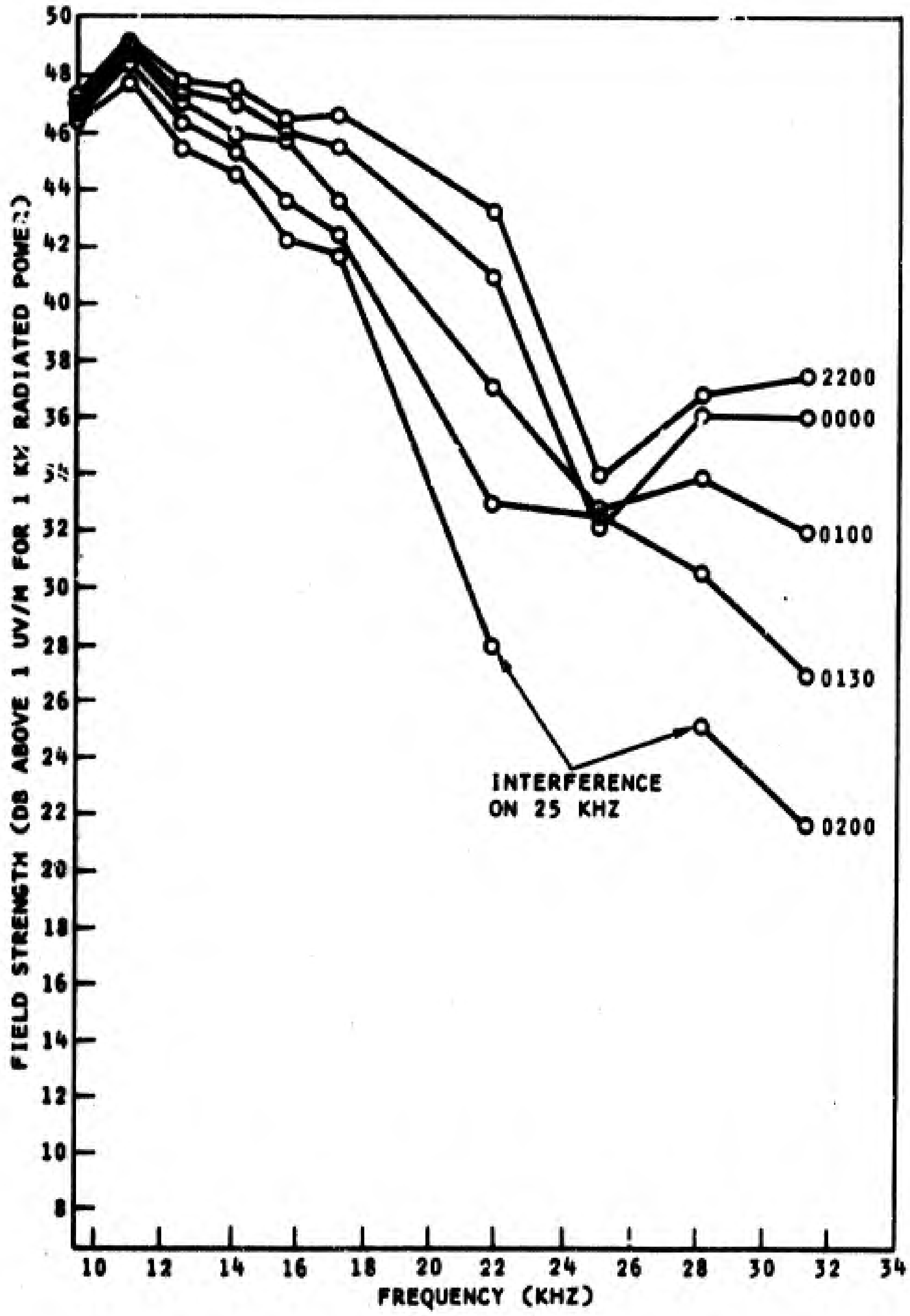

FIG. 21. Experimental Values of Field Strength vs. Frequency from Noon to Sunset on 13 March 1967.

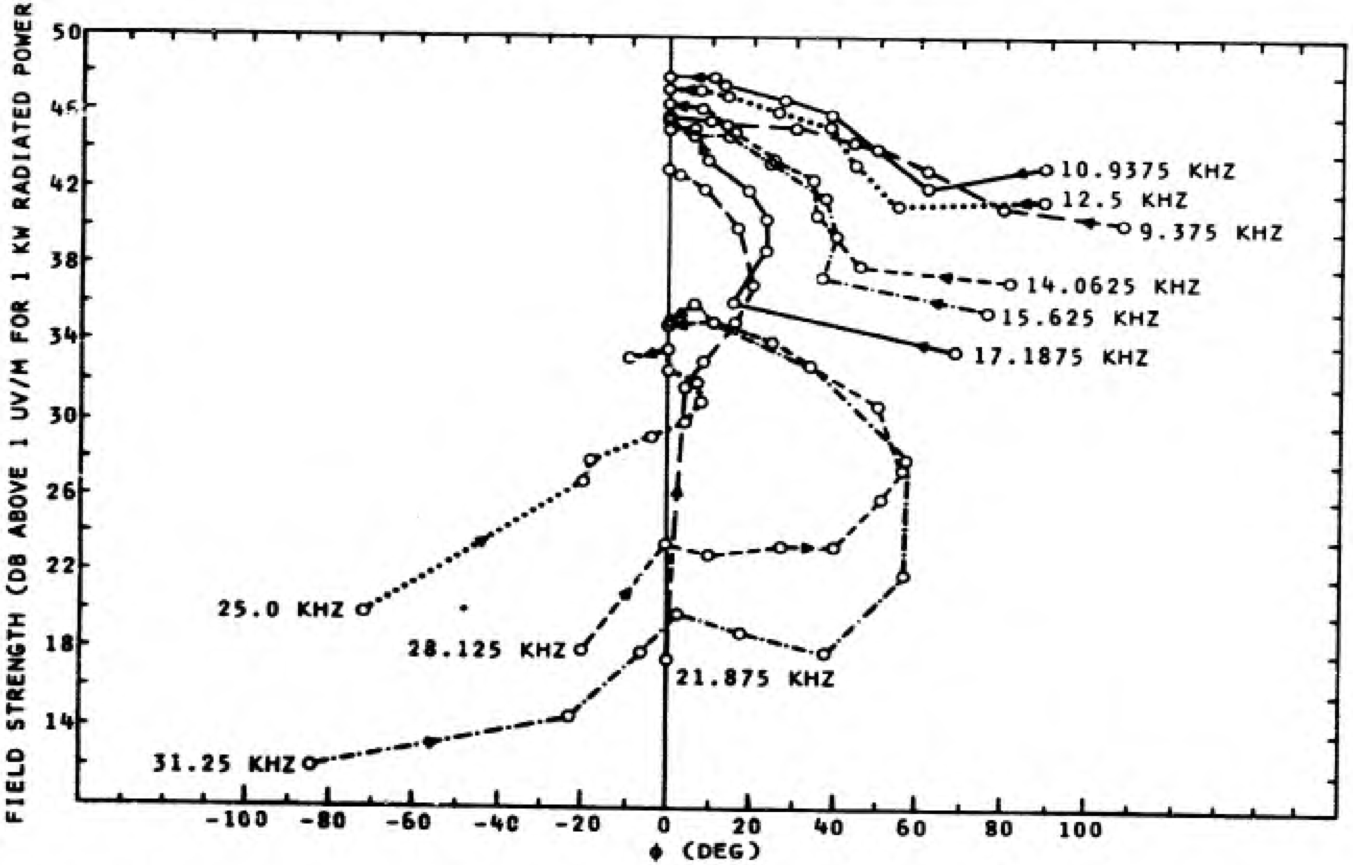

FIG. 22. Experimental Values for Field Strength vs. Phase for Sunrise to Noon on 7 March 1967 (Phase measured relative to phase at 2130 U.T.).

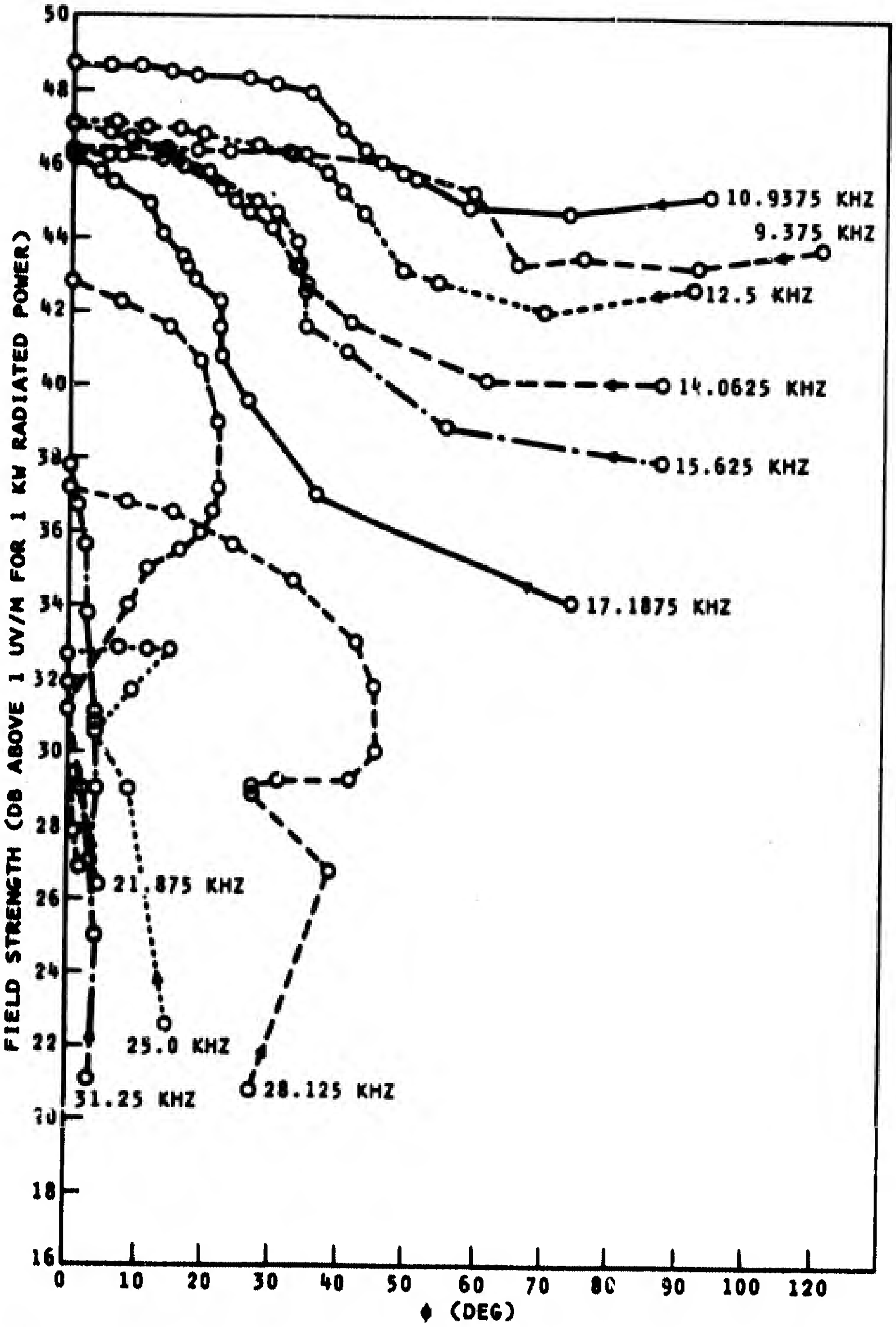

FIG. 23. Experimental Values for Field Strength vs. Phase for Sunset to Noon on 14 March 1967 (Phase measured relative to phase at 2130 U.T.).

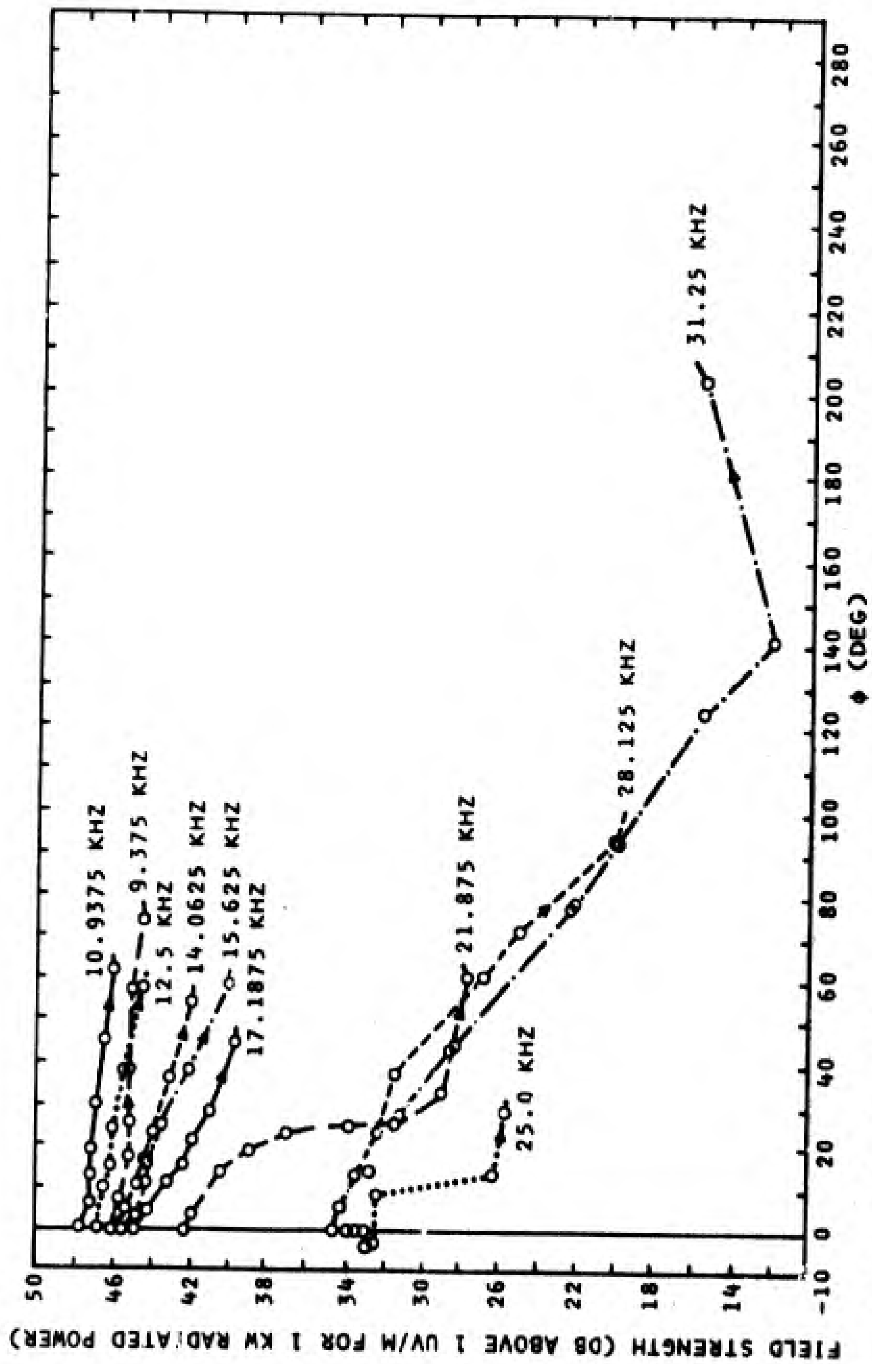

FIG. 24. Experimental Values for Field Strength vs. Phase for Noon to Sunset on 6 March 1967 (Phase measured relative to phase at 2130 U.T.).

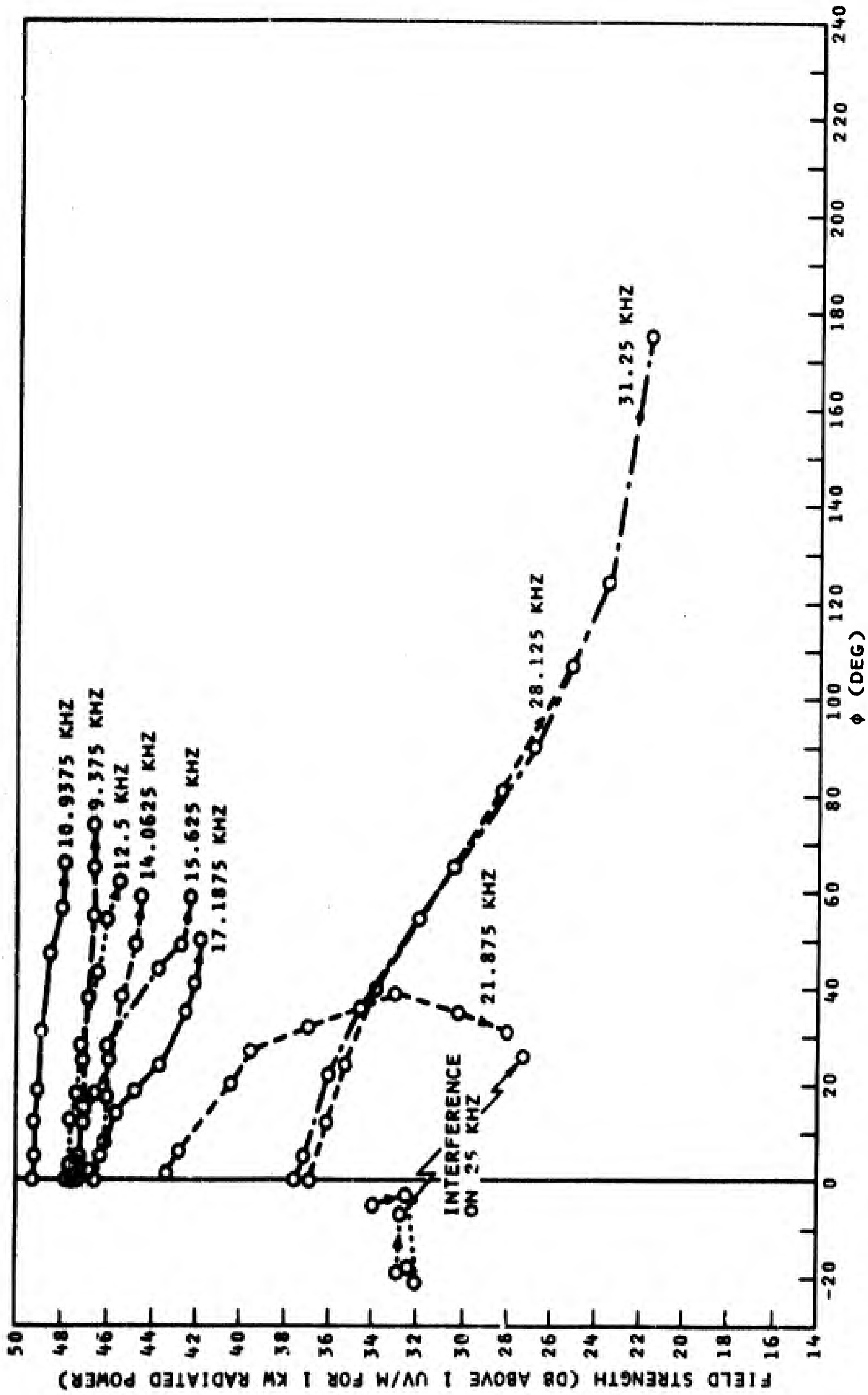

FIG. 25. Experimental Values for Field Strength vs. Phase for Noon to Sunset on 13 March 1967 (Phase measured relative to phase at 2130 U.T.).

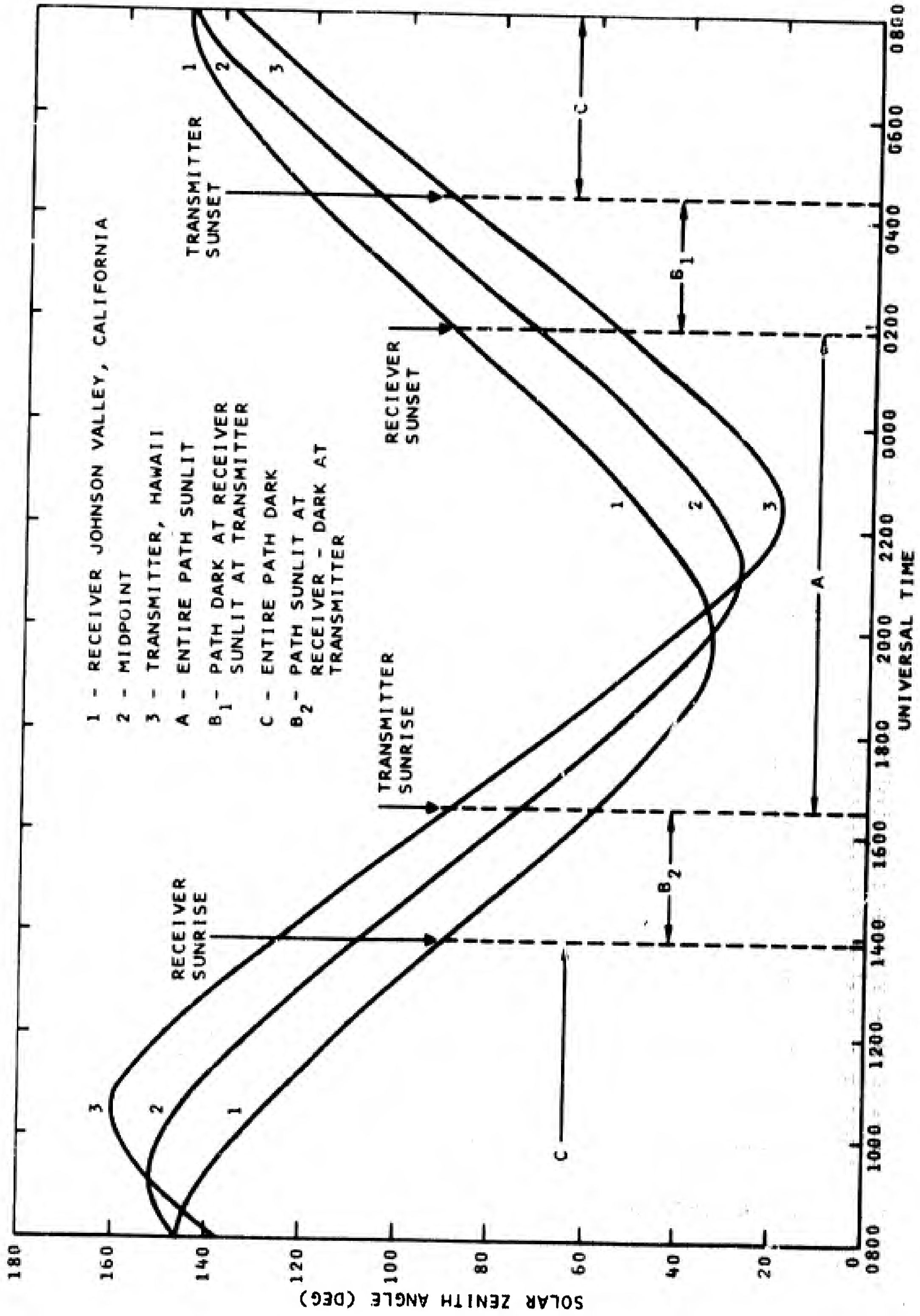

FIG. 26. Solar Zenith Angle vs. Time for 21 March 1967.

deriving profiles for other times is somewhat dependent upon the accuracy of the reference profile. Interestingly, attempts to derive profiles for other times have led to improvements in the reference profile. It is noted in Fig. 22 and 24 that the time variability of the signals is different for the morning and afternoon periods. It is now evident that an ionization shelf, previously referred to by other investigators as a C layer, is formed early in the morning at an altitude near 65 km and that as the morning progresses the region above this shelf is gradually filled in, eventually forming the noon time profile. A series of electron profiles is presented in Fig. 27 to show in a general way this time variability. It is to be emphasized that the profiles of Fig. 27 do not correlate in detail with a specific set of propagation data. The ionosphere relaxation during the afternoon appears to progress in a different manner. In this case attempts to find a match between observation and a suitable series of profiles have proven to be even more difficult. The observed phase change would indicate a raising of the total ionosphere, including the C layer. Such raising is difficult without a corresponding increase in the fields of the lower frequencies, which is not observed in the data. A continuing effort is being made to derive explicit profiles from the propagation data for both the morning and afternoon periods.

DISCUSSION

As stated in the Introduction, the established objectives of this evaluation project were (1) to determine the degree of correlation obtainable between the experimental data and model prediction, (2) to determine the variability of propagation parameters derived from the experimental data, and (3) to compare with previously published findings the theoretical model parameters which best describe experimental results. Even though the progress which has been made is considered significant, these objectives have not yet been fully achieved. The achievements and difficulties related to these project objectives will now be discussed.

Very good agreement has been achieved in a few specific instances between the experimental data and the prediction of received fields from an assumed propagation model. The ability to derive a propagation model with which to describe experimental results has generally been disappointingly poor, however. Since these difficulties have not been traceable to deficiencies which would reduce the credibility of the model, it is assumed that these difficulties result from the complexities of the method for deriving the model parameters. Undoubtedly,

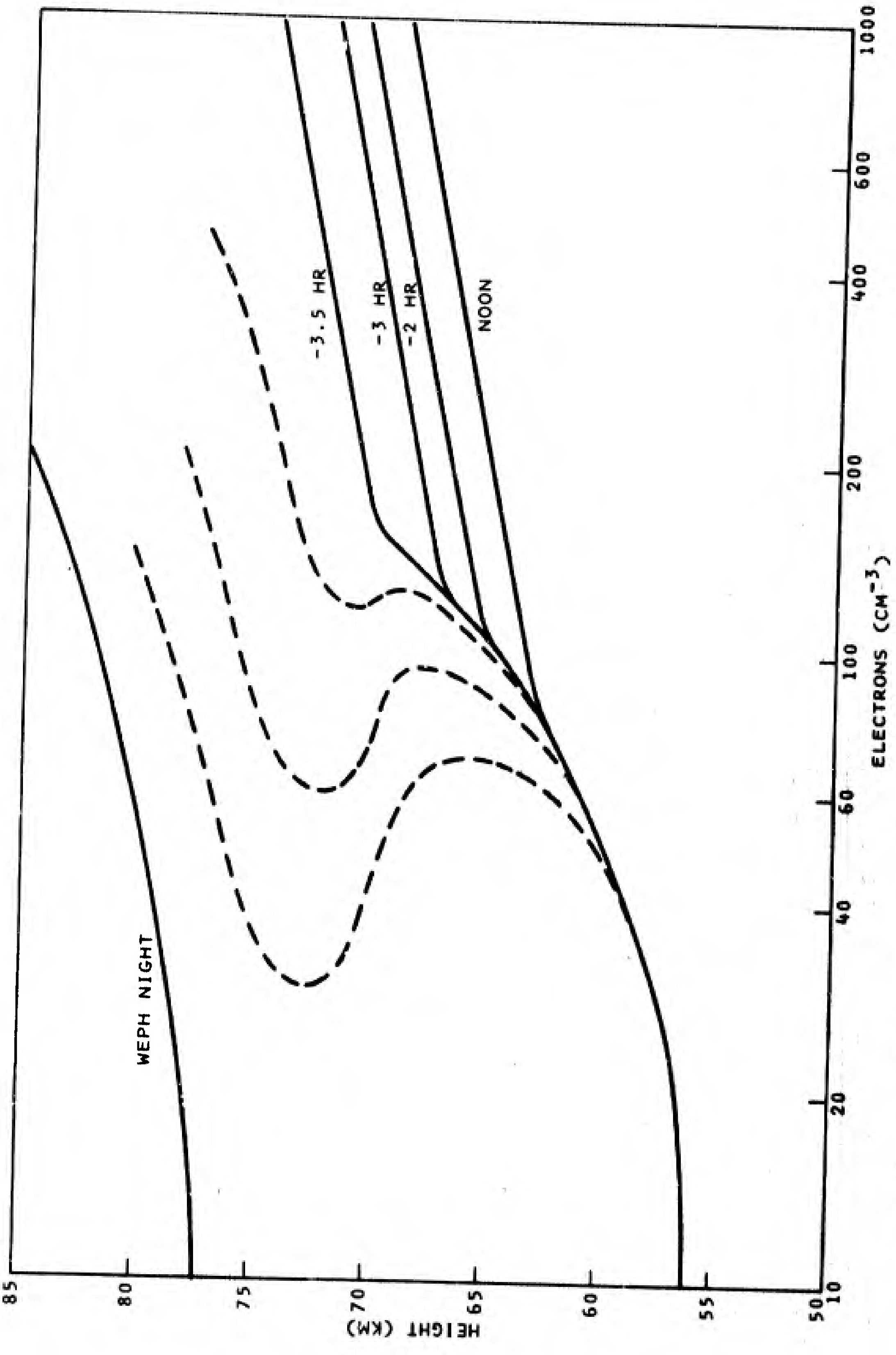

FIG. 27. Predicted Electron Density Profiles for Sunrise to Noon on 7 March 1967.

a good share of the difficulty must be attributed to the lack of experience in selecting model parameters. The trial and error process of selecting the electron density profile to be used in the model dictates that additional information be obtained concerning the relationships between the properties of the profile and the resulting fields at the receiving terminator of a path. The problem is further complicated by the fact that the measurement precision required to evaluate a choice of an electron profile taxes the present measurement capability. Improvements are now being made in the measurement technique which will greatly facilitate the comparison of experimental data with model predictions. The discussion of these techniques is appropriately left to a future report.

Some of the specific continuing discrepancies between experimental measurement and model prediction are as follows. First, the received fields as measured were consistently higher by approximately 3 dB, than those predicted by any propagation models. A reevaluation of both computational techniques and measurement techniques has not resulted in an explanation of this discrepancy. Recently, a comparison has been made between calculations made at the NWC Corona Laboratories and those made with a WAVEGUIDE computer code at the Naval Electronics Laboratory Center, San Diego (Ref. 16). The agreement between these calculations would indicate that this 3 dB discrepancy probably results from the measurement technique. This possibility will be investigated further. Second, more variability has been observed in the relative signal levels between the four lowest frequencies than has been derivable from any assumed electron density profile. Again, this could be a measurement problem. It is known that the measurement of the radiated field with a ground wave receiver (used to calibrate the transmissions) is contaminated by the incident one hop sky wave. This contamination, which decreases with increasing frequency, is theoretically of about the same magnitude as the discrepancy between the experimentally measured received fields over the oblique path and the predicted fields. This discrepancy, which is generally less than 1 dB, is not resolvable with the present measurement data. If this variability results from the ionosphere, one may have a lead with which to examine localized irregularities. In future measurements, the sky wave contamination of the radiated power calibration will be eliminated with special receiver gating. Third, a consistent discrepancy has existed between the predicted fields for the 31.25 kHz signal and the measured signal, the measured signal being lower in amplitude than that predicted for the model giving a best fit with the measured values at all other frequencies. Again, no explanation has been derived, even though a very careful check has been made of the measurement procedure. Fourth, a good profile match has not been achieved for the early morning or late afternoon propagation environment. The derivation of this profile is highly dependent upon establishment of a high quality reference profile near the midpath noon period. The reason is that without absolute phase information, the profile height cannot be determined except at times when sufficient modal interference structure exists to establish a measurable height dependent relationship in the amplitudes of the higher frequencies. This condition occurs only near the middle of the day, as at other times the higher ionosphere loss eliminates the measurable mode structure. Once a good reference profile is established utilizing the mode structure data, use can be made of phase changes with time from this reference point to accurately define the profile at times when the ionosphere parameters are such as to rapidly attenuate higher ordered modes. The profiles for the very early morning or very late afternoon are best derived with a sequence of matches between experimental data and computed models at incremental time intervals between the reference profile time and a time for which the final match is desired. This sequential matching consumes considerable computer time and involves considerable effort. Much more experience will be required to refine this technique.

With regard to determining the variability of propagation parameters, a number of qualitative observations are worth discussing. First, the profiles derived which best represent noonday propagation for this path produce, generally speaking, less propagation loss and more mode structure than that traditionally used for daytime models. The degree to which the mode structure increases the increasing ionosphere gradient is illustrated in Fig. 28. Reference is also made to Fig. 9 to illustrate the differences in signal characteristics produced by different ionosphere gradients. Second, the electron density profile derived (see Fig. 15 for example) deviates significantly from an exponential form. Third, the variability in the noontime profile very closely follows the variability in solar activity for the period of measurement. The variability of the electron density profile with variations in solar activity for electron density values above approximately 100 el/cm^3 and the relative stability of the profile at densities below the value of 100 el/cm^3 is quite well established from the data analysis that has been undertaken. Even though only three profiles are presented in Fig. 15, the data of Fig. 14 shows a consistent pattern of changes for five separate dates. Without question, though, additional experimental data to support this observation would be most valuable, particularly if x-ray radiation data from satellites could be acquired for correlation

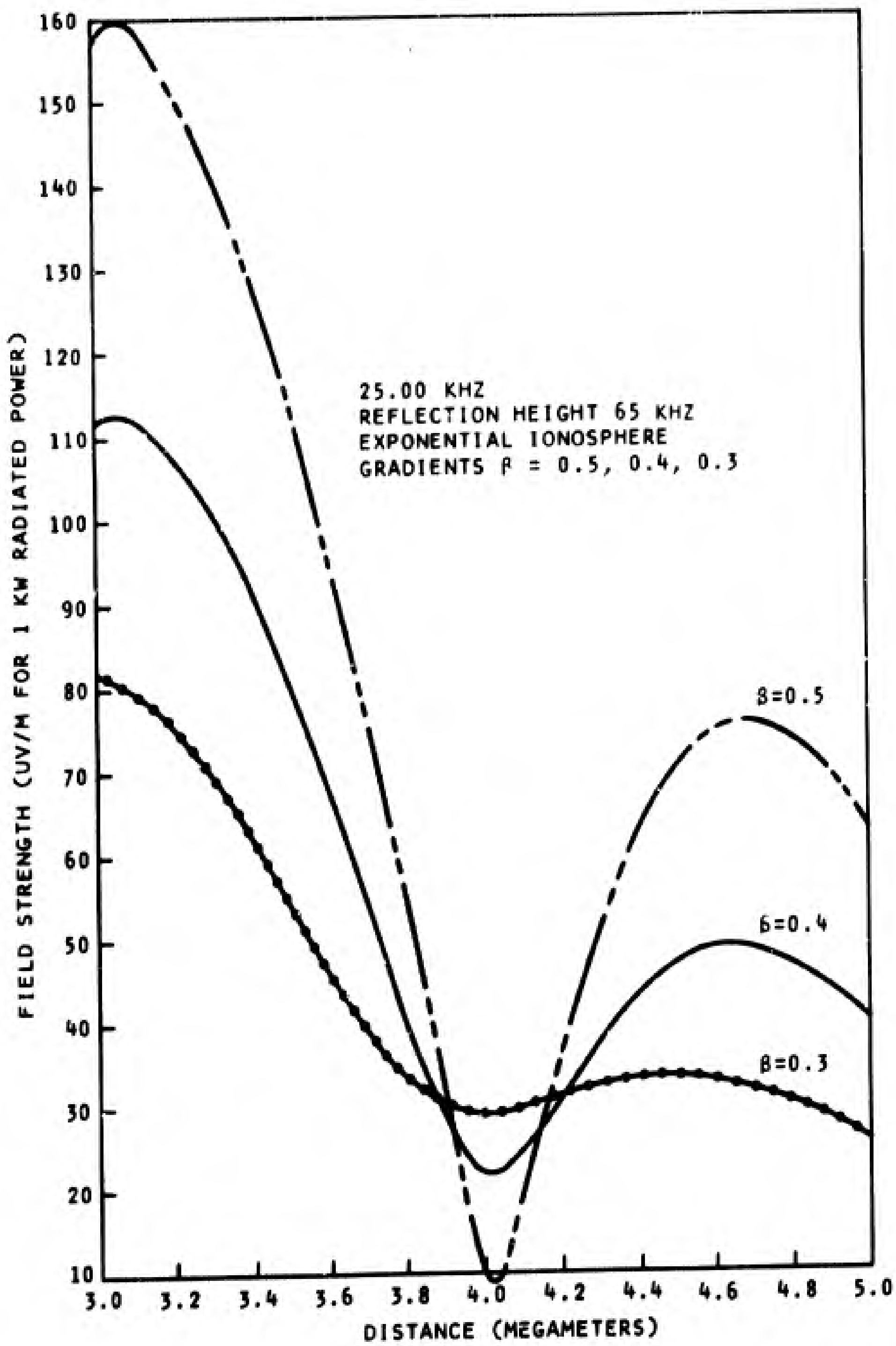

FIG. 28. Field Strength vs. Range at 25 kHz Showing the Increase in Modal Structure Associated with an Increasing Gradient of the Electron Density Profile.

purposes. Fourth, a direct relationship is evident between the profile and the solar zenith angle from the data presented in Fig. 18-25, even though the specific profiles to demonstrate this relationship have not been acquired. It is also evident that a significant variation in ionosphere profiles would exist due to the seasonal effect, since the noon solar zenith angle, which is 32° for 21 March, can vary through the season from 55-1/2° to 18-1/2°. (A midpath solar zenith angle of 55° occurs at approximately 1800 and 0030 on 21 March.) This data would also indicate that the profile parameters would change significantly with geographic latitude.

Needless to say, only a small beginning has been made toward establishing the degree of variability of propagation profile parameters. Good evidence has been acquired, however, to indicate that at least at low latitudes the electron density profile is variable in a potentially predictable way. The established continuous variability of the profile with variations in solar zenith angle makes it evident that the profiles which produce a good match for experimental data over the 4,166-km path would not produce a good match for a significantly longer path, say on the order of 6,000 to 8,000 km. Thus, the question is still very open as to whether a single representative profile can be used in a propagation model to adequately describe propagation over a very long VLF path, even assuming total daylight. In fact, there is some suspicion that the difficulties in obtaining a satisfactory match to explain the early morning or late afternoon propagation environments may be due to the fact that the path cannot be precisely represented by an equivalent constant height ionosphere having a fixed profile for the total path. Proving the model inadequate may be a very difficult task. The most logical test at this time appears to be to utilize the data acquired on a relatively short path, say 3,000 to 4,000 km, to derive the model parameters for predicting fields for a longer path, say 6,000 km, and then to compare the data received at 6,000 km with the predictions.

The electron density profiles which have been derived for the midday deviate significantly from those that have been published in previous literature. This in itself is not unexpected in that the variations between published profiles is as great as the deviations of the Corona Laboratories profile from any given previously published profile. The evaluation of a computational technique includes a determination as to whether the input parameters required to derive agreement with experimental observation are physically realistic. Neither a direct measurement of electron density profile nor an independent assessment of its properties were made during the time in which the propagation measurements were obtained. Thus, one is limited to evaluating the likelihood of the profile derived with the model. One step in this evaluation is to make a comparison between published profiles derived from theoretical concepts and/or direct experimental measurement. Unfortunately, in many instances where investigators have considered or measured the properties of the D-region ionosphere, consideration was not given to the altitude region and/or the electron density range of greatest importance to VLF propagation. Another problem is that much of the measurement data has been taken at very high latitudes such as Fort Churchill and Ottawa in Canada and Kiruna, Sweden. A representative sample of profiles which have been acquired from the literature is presented in Fig. 29(a), (b), and (c). Ionosphere I is the β = 0.3 profile used by Wait (Ref. 9). Ionosphere II is an exponential profile with β = 0.5 used by Rhodes and Garner (Ref. 17). Profile III, which was published by Deeks (Ref. 10), was found to be representative of summer noon for solar sunspot minimum. The solar zenith angle for this condition would be approximately 28°. Profile IV, provided by John Bickel (Ref. 16), is considered as representative of conditions for a large sample of VLF propagation data. Profile V was derived from computations made by Moler (Ref. 18) for a solar zenith angle of 0° and a geomagnetic latitude of 3°. The dotted profile extension which has been added represents the estimated additional ionization produced by cosmic rays for a geomagnetic latitude of 51°, again based upon Moler. Profile VI, published by Smith (Ref. 19), represents an electron density profile for a solar zenith angle of 15-1/2° in Australia as acquired by partial reflection measurement techniques. Profile VII was published by Baybulatov and Krasnushkin (Ref. 20). In these figures the profile marked NWC is that acquired at the Corona Laboratories for 7 March, noon. An interpretation of the differences between these profiles has not been made. Some interesting observations, however, are as follows. The NWC profile lies generally between the β = 0.3 and β = 0.5 profiles (Fig. 29(a)). Profile VII has a shape closest to that of the NWC profile, but with a somewhat larger C layer component (that is, from 10-100 el/cm^3), and a generally higher level at values above 100 el/cm^3. Considerable intercomparison was made between experimental propagation data obtained with the sounder and profiles published by Deeks. The S-shaped region in the Deeks profile simply produces too great a path loss and insufficient mode structure to produce a good fit with the propagation data.

The question arises as to the uniqueness of the NWC profile. It is very difficult to make a definitive statement concerning this uniqueness. It can be stated unequivocally, however, that none of the other profiles

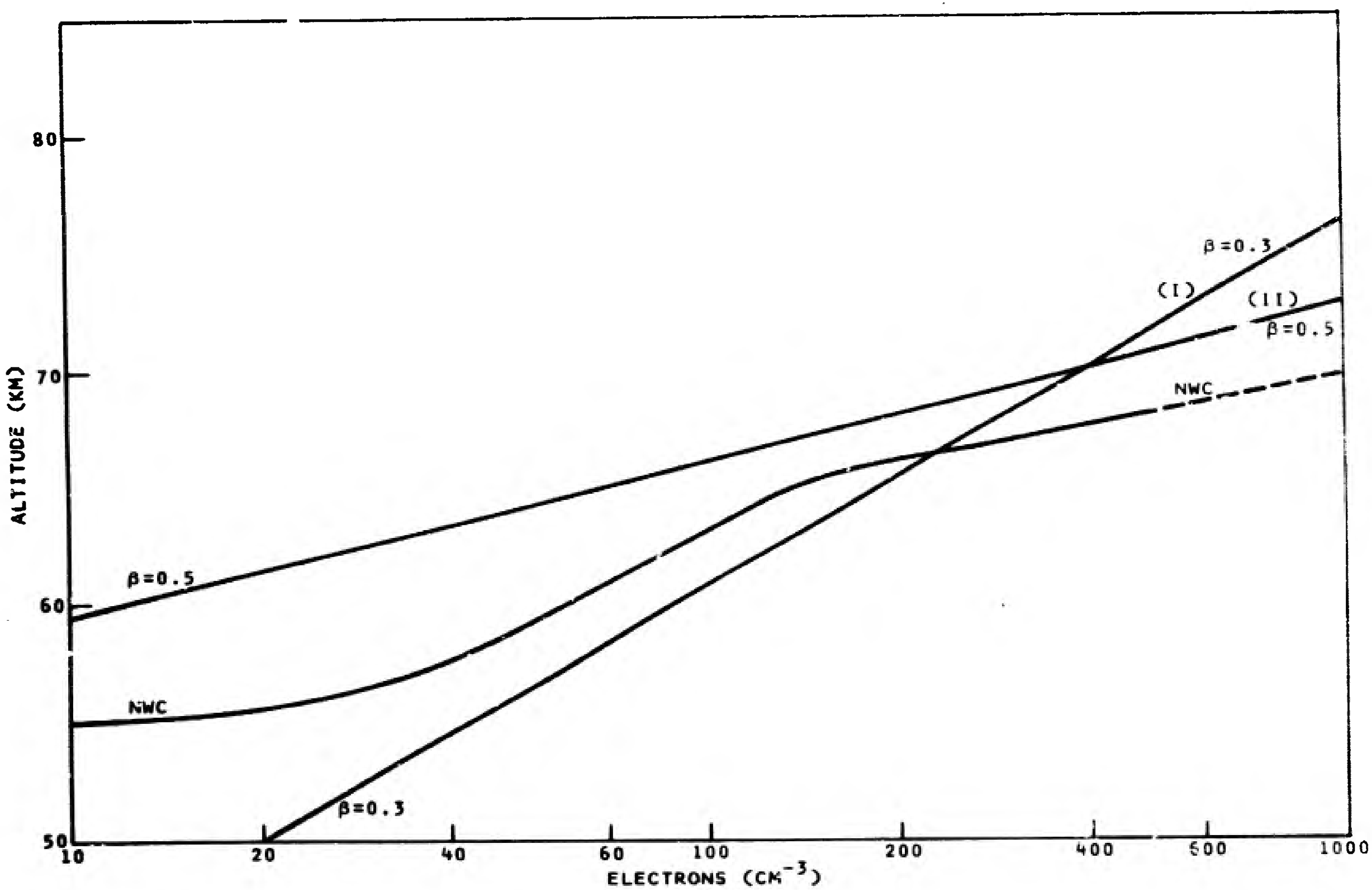

FIG. 29(a). Electron Density Profiles Taken from Existing Literature.

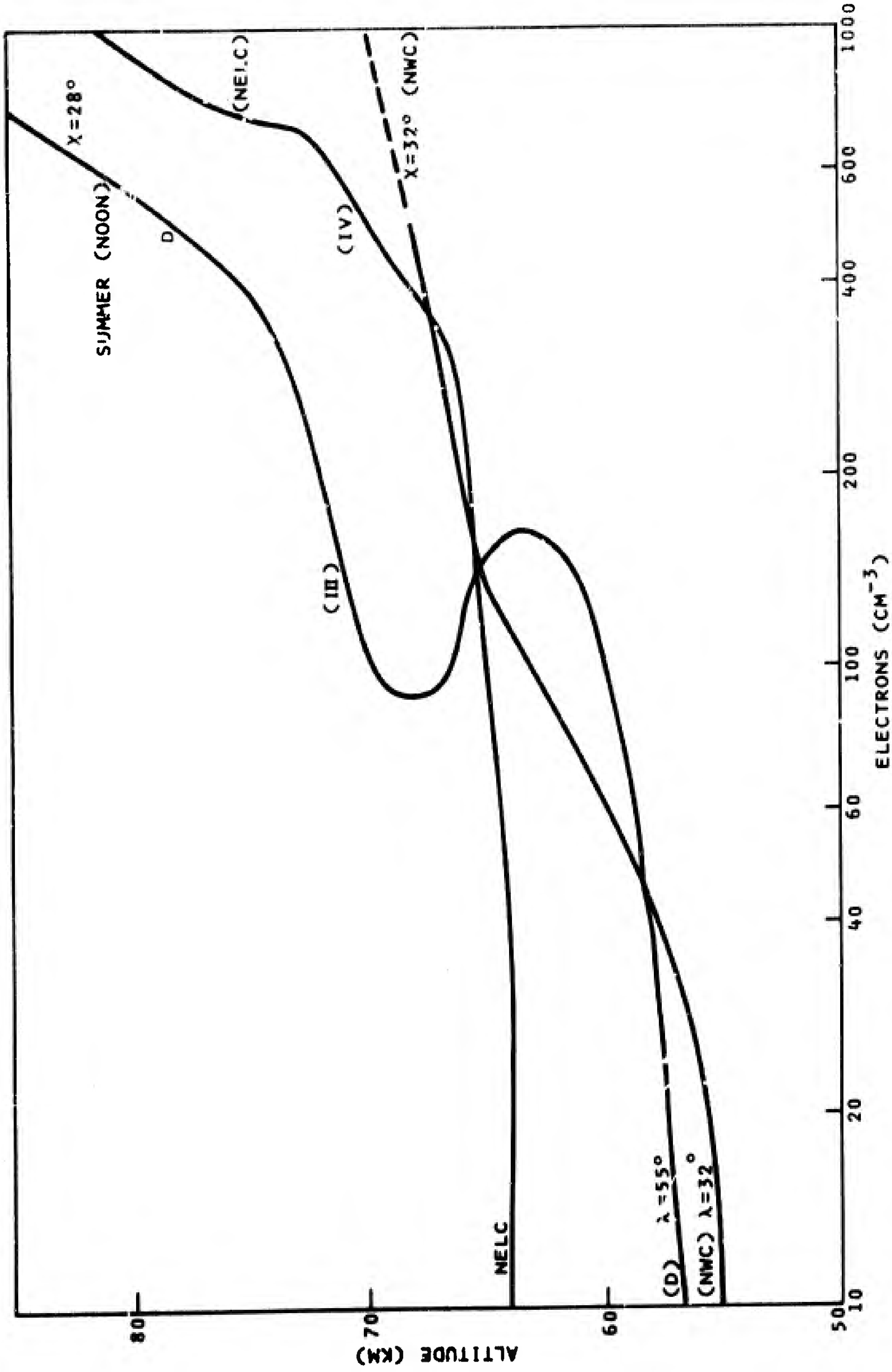

FIG. 29(b). Electron Density Profiles Taken from Existing Literature.

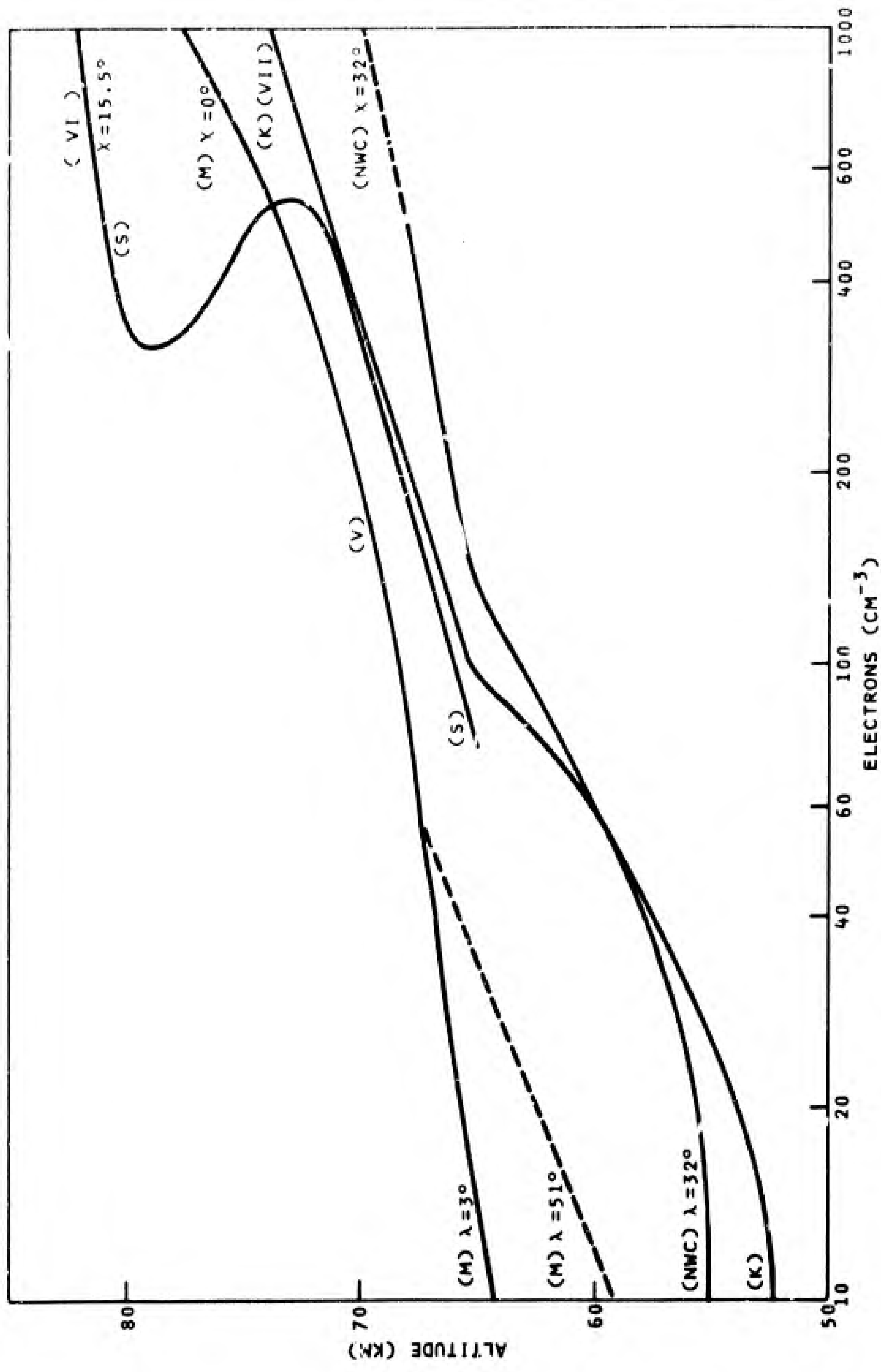

FIG. 29(c). Electron Density Profiles Taken from Existing Literature.

presented in Fig. 29 adequately describe the experimental data. Details of the shape of the NWC profile such as the particular curvature selected for the profile region between the densities of 10 el/cm^3 and 150 el/cm^3 and the exponential gradient between 150 el/cm^3 and 500 el/cm^3 can probably be justified as the simplest form which provides an adequate match with the experimental data. Probably the major limitation on determining the uniqueness of the data at this time is the accuracy limitations of the experimental measurements. Experience at attempting to derive profiles would indicate that the combined values of amplitude and phase data for 10 frequencies place a very tight limitation on the choices of a profile. In summary, the fact that absolute phase data was not obtained and the fact that establishment of the received fields is limited to about 1/2 dB does allow for some indetermination in the profile shape.

A definitive conclusion on the physical possibility of a profile derived from the propagation measurements was not obtainable from comparisons with published data primarily because of the wide variation in published profiles. Because of this, any additional clues for determining the credibility of the derived profile were considered very valuable. The consistency of the relationships between variations in solar activity and solar position have been a great aid in establishing confidence that the profiles derived are a very good representation of physical conditions. In fact, it is now expected that this measurement technique, in conjunction with the theoretical model, will make it possible to obtain a more definitive measure of that portion of the electron density profile important to long path VLF propagation than most other experimental techniques that have been devised.

CONCLUSIONS

Most of the progress that has been made to date in this project must be classified as demonstrating the potential for achieving the objectives outlined. The conclusions that can be drawn from this effort are thus primarily in the form of defining further refinements to the techniques, although the initial findings have important ramifications. It has been well established that the multiple frequency propagation data can provide a wealth of information concerning the propagation environment and that it is possible to quite precisely establish the propagation parameters. With respect to measurement techniques, it is evident that a high degree of measurement precision is required to define the detail desired. It is also evident that the ability to define parameters would be greatly enhanced if the values of the received signals could be precisely referenced to transmitter radiations. Steps are now being taken to improve the measurement capability through a more accurate measurement of transmitter radiation and utilization of a modulation scheme to tie the received phase measurements to the transmitted signal phases. Consideration is also being given to using a transportable clock to establish precise time between the transmitting and receiving sites. An additional measurement capability now being evaluated as part of an Office of Naval Research project is to use two receiving terminals so located as to take optimum advantage of the modal constructive and destructive interference variation between frequencies. Such a technique is expected to make it possible to precisely establish the parameters of the propagation media without requiring a precise measure of transmitted signal, time, and geographic relationship between the transmitter and receiver sites. With respect to computer computations, further evaluation is required to determine the importance of being able to include the very low density portion of the profile (that is, values between 0 and 10 el/cm^3) in the modeling computations. Equally important, it has become very evident that the process of matching electron profile models to experimental data is extremely cumbersome and, because of the large amount of computer time involved, expensive. Much encouragement should be given to the development of an analytical process for deriving best fit electron density profiles from experimental data. Finally, the measurement findings show evidence of very high stability in the propagation media which is in agreement with previous observations, but also a high variability in the propagation parameters with solar time and it is assumed with geographic latitude and the season. These findings, which should be confirmed by additional measurements, do raise many questions relevant to the modeling requirements for the daytime ambient propagation media. The questions that have arisen are most immediately applicable to general Navy VLF communications problems, particularly in the establishment of communications coverage charts, and the development of propagation prediction techniques. However, they also have relevance to the development of analytical models for handling the highly disturbed environment in that they should provide considerable insight as to the limitations which may be imposed by the concept of a uniformly disturbed ionosphere—that is, one in which the profile is invariant over the total length of the path.

REFERENCES

1. Naval Ordnance Laboratory, Corona. Multiple-Frequency Oblique-Incidence VLF Ionospheric Sounder, by V. E. Hildebrand and D. A. Wulfing. Corona, Calif., NOLC, 5 May 1967. (NOLC Report 722)

2. ——————. Broad-Band VLF Transmitting Stagger-Tuned Dipole, by E. W. Seeley and D. A. Wulfing. Corona, Calif., NOLC, 18 May 1966. (NOLC Report 653)

3. ——————. Horizontal VLF Transmitting Antennas Near the Earth, by E. W. Seeley and P. H. Wiborg, Jr. Corona, Calif., NOLC, 15 May 1967. (NOLC Report 721)

4. ——————. The Two-Loop Superdirective End-Fire Antenna, by E. W. Seeley. Corona, Calif., NOLC, 1 April 1962. (NOLC Report 562)

5. Wait, J. R. "A Note on Diurnal Phase Changes of Very-Low-Frequency Waves for Long Paths," J GEOPHYS RES, Vol. 68 (January 1963), pp. 338-340.

6. Blackband, W. T. "Diurnal Changes in the Time of Propagation of VLF Waves Over Single Mode Paths," in Propagation of Radio Waves at Frequencies Below 300 kc/s, ed. by W. T. Blackband. New York, Macmillan, 1964. Pp. 219-229.

7. National Bureau of Standards Boulder Laboratories. Fortran Programs for Full-Wave Calculation of LF and VLF Radio Propagation, by L. A. Berry and M. A. Chrisman. Boulder, Colo., NBS Boulder Laboratories, 11 October 1965. (NBS Report 8889)

8. Air Force Cambridge Research Laboratories. Numerical Solution of Full-Wave Equation with Mode-Coupling, by Yuji Inoue and Samuel Horowitz. L. G. Hanscom Field, Bedford, Mass., AFCRL, February 1966. (AFCRL-66-114, Physical Science Research Papers, No. 196)

9. National Bureau of Standards Boulder Central Radio Propagation Laboratory. Characteristics of the Earth-Ionosphere Waveguide for VLF Radio Waves, by J. R. Wait and K. P. Spies. Washington, D. C., Government Printing Office, 30 December 1964. (NBS Technical Note No. 300)

10. Deeks, D. G. "The D-Region Electron Distributions in Middle Latitudes Deduced from the Reflection of Long Radio Waves," ROY SOC LONDON, PROC, SER A, Vol. 291 (1966), pp. 413-437.

11. Jean, A. G., H. E. Taggart, and J. R. Wait. "Calibration of Loop Antennas at VLF," NAT BUR STAND, J RES, SECT C, ENG AND INSTR, Vol. 65 (July-September 1961), p. 189.

12. Department of Commerce Environmental Science vices Administration. Solar-Geophysical Data. Washington, D. C., September 1967. (IER-FB-277)

13. Bowling, T. S., K. Norman, and A. P. Willmore. "D-Region Measurements During a Solar Eclipse," PLANETARY SPACE SCI, Vol. 15 (1967), pp. 1035-1047.

14. White, W. A. "Solar X-Rays: A Comparison with Microwave Radiation," in AAS-NASA Symposium on the Physics of Solar Flares. Greenbelt, Md., Goddard Space Flight Center, 1964. (NASA SP-50)

15. Kreplin, R., Naval Research Laboratory, Washington, D. C., private communication.

16. Bickel, J. E., Naval Electronics Laboratory Center, San Diego, Calif., private communication.

17. Naval Research Laboratory. An Investigation of the Modal Interference of Very-Low-Frequency Radio Waves, by F. J. Rhoads and W. E. Garner. Washington, D. C., NRL, 27 October 1965. (NRL Report 6359)

18. Moler, W. F. "VLF Propagation Effects of a D-Region Layer Produced by Cosmic Rays," J GEOPHYS RES, Volume 65 (May 1960), pp. 1459-1468.

19. Air Force Cambridge Research Laboratories. Radio Wave Interaction Using Gyro-Waves, by R. A. Smith, I. A. Bourne, R. G. Loch, C. S. G. K. Setty, T. N. R. Coyne, P. H. Barratt, and B. S. N. Prasad. L. G. Hanscom Field, Bedford, Mass., AFCRL, 17 June 1965. (AFCRL-65-460, Scientific Report No. 3)

20. Baybulatov, R. B., and P. Ye. Krasnushkin. "Determination of the Daytime Electron Concentration Profile of the C and D Layers of the Ionosphere from the Measurements of the Surface Fields of Ultralong Radio Waves and from the Atmospheric Pressure Profile," GEOMAGNETISM AND AERONOMY, Vol. VI, No. 6 (1966), pp. 819-827.

Security Classification UNCLASSIFIED

DOCUMENT CONTROL DATA - R & D

(Security classification of title, body of abstract and indexing annotation must be entered when the overall report is classified)

1. ORIGINATING ACTIVITY *(Corporate author)* Naval Weapons Center Corona Laboratories	2a. REPORT SECURITY CLASSIFICATION UNCLASSIFIED 2b. GROUP

3. REPORT TITLE

AN EVALUATION OF VLF DAYTIME PROPAGATION PARAMETERS USING A MULTI-FREQUENCY SOUNDER

4. DESCRIPTIVE NOTES *(Type of report and inclusive dates)*

5. AUTHOR(S) *(First name, middle initial, last name)*

Verne E. Hildebrand
David G. Morfitt

6. REPORT DATE	7a. TOTAL NO. OF PAGES	7b. NO. OF REFS
30 March 1968	77	20

8a. CONTRACT OR GRANT NO. b. PROJECT NO. c. Defense Atomic Support Agency MIPR 518-68 d.	9a. ORIGINATOR'S REPORT NUMBER(S) NWCCL TP 759 9b. OTHER REPORT NO(S) *(Any other numbers that may be assigned this report)*

10. DISTRIBUTION STATEMENT

THIS DOCUMENT IS SUBJECT TO SPECIAL EXPORT CONTROLS AND EACH TRANSMITTAL TO FOREIGN GOVERNMENTS OR FOREIGN NATIONALS MAY BE MADE ONLY WITH PRIOR APPROVAL OF THE COMMANDING OFFICER OF THE NAVAL WEAPONS CENTER CORONA LABORATORIES (CODE 2035), CORONA, CALIFORNIA 91720.

11. SUPPLEMENTARY NOTES	12. SPONSORING MILITARY ACTIVITY
	Defense Atomic Support Agency

13. ABSTRACT

An oblique incidence VLF ionospheric sounder system ~~developed at the Naval Weapons Center Corona Laboratories~~ gives a means of obtaining multi-frequency amplitude and phase measurements in the VLF band simultaneously at up to 10 frequencies over a single propagation path. The analysis presented in this report is an attempt (1) to determine the degree of correlation obtainable between experimental sounder data and predicted results from existing theoretical models for VLF propagation, (2) to determine the variability of propagation parameters derived from the experimental data, and (3) to compare theoretical model parameters which best describe experimental results with previously published findings.

DD FORM 1 NOV 65 1473 (PAGE 1)

S/N 0101-807-6801

UNCLASSIFIED
Security Classification

Security Classification UNCLASSIFIED

14. KEY WORDS	LINK A		LINK B		LINK C	
	ROLE	WT	ROLE	WT	ROLE	WT
Ionosphere						
D-Region						
Electron density profiles						
Multi-frequency oblique incidence VLF ionospheric sounder						
Amplitude of propagated signal						
Phase of propagated signal						
VLF-propagation parameters						
VLF-propagation path						
Computerized data processing						
Theoretical propagation models						
Isotropic propagation						
Anisotropic propagation						
Transmission coefficient						
Reflection coefficient						
Reflection height						
Modal structure						

DD FORM 1 NOV 65 1473 (BACK)
(PAGE 2)

UNCLASSIFIED
Security Classification

AD 829 842

17 April 1968

ERRATA

Naval Weapons Center Corona Laboratories. AN EVALUATION OF VLF DAYTIME PROPAGATION PARAMETERS USING A MULTI-FREQUENCY SOUNDER, by V. E. Hildebrand and D. G. Morfitt. Corona, Calif., NWC Corona Laboratories, March 1968. (NWCCL TP 759)

On page 1, paragraph 2, line 4, change "low-altitude" to "low-latitude."

On page 7, in the legend for Fig. 3(b), change "14.6" to "14.06."

On page 9, line 14, change "21.125" to "21.875."

On page 15, line 9, change the word "reception" to "reflection."

On pages 17, 18, and 19, in the legends for Fig. 5(a), 5(b), and 5(c), change the word "Frequency" to "Distance."

On pages 17, 18, and 19, in the small graphs which appear in the upper right hand corners of Fig. 5(a), 5(b), and 5(c), change the horizontal scale label from "ELECTRONS (CM^{-1})" to "ELECTRONS (CM^{-3})."

On page 43, change the vertical scale label of Fig. 18 from "FIELD STRENGTH (DB ABOVE 1 UV/M FOR RADIATED POWER)" to "FIELD STRENGTH (DB ABOVE 1 UV/M FOR 1 KW RADIATED POWER)."

On page 46, in Fig. 21, add the words "UNIVERSAL TIMES" above the notation "2200."

On page 48, in the legend for Fig. 23, change the word "Sunset" to "Sunrise."

AD 829842

13 August 1968

ADDITIONAL ERRATA

Naval Weapons Center Corona Laboratories. AN EVALUATION OF VLF DAYTIME PROPAGATION PARAMETERS USING A MULTI-FREQUENCY SOUNDER, by V. E. Hildebrand and D. G. Morfitt. Corona, Calif., NWC Corona Laboratories, March 1968. (NWCCL TP 759)

On page 38, the vertical scale value for the 7 March data should be changed from 45.4 to 45.9.

On page 43, all of the values on the vertical scale should be increased by 2 dB; i.e., the highest value should be 48 dB and the lowest value should be 12 dB.